Proton Donor in Yeast Pyruvate Kinase: Chemical and Kinetic Properties of the Active Site Thr 298 to Cys Mutant†

Delia Susan-Resiga and Thomas Nowak*

Department of Chemistry and Biochemistry, University of Notre Dame, Notre Dame, Indiana 46556

Received January 16, 2004; Revised Manuscript Received September 16, 2004

ABSTRACT: The active site T298 residue of yeast pyruvate kinase (YPK), located in a position to serve potentially as the proton donor, was mutated to cysteine. T298C YPK was isolated and purified, and its enzymatic properties were characterized. Fluorescence and CD spectra indicate minor structural perturbations. A kinetic analysis of the Mg^{2+}-activated enzyme demonstrates no catalytic activity in the absence of the heterotropic activator fructose 1,6-bisphosphate (FBP). In the presence of Mg^{2+} and FBP, T298C has approximately 20% of the activity of wild-type (wt) YPK. The activator constant for FBP increases by 1 order of magnitude compared to this constant with the wt enzyme. T298C shows positive cooperativity by FBP with a Hill coefficient of 2.6 (wt, $n_{H,FBP} = 1$). Mn^{2+}-activated T298C behaves like Mn^{2+}-activated wt YPK with a V_{max} that is 20% of that for the wt enzyme with or without FBP. A pH−rate profile of T298C relative to that for wt YPK shows that p$K_{a,2}$ has shifted from 6.4 in wt to 5.5, indicating that the thiol group elicits an acidic pK shift. Inactivation of both wt and T298C by iodoacetate elicits a pseudo-first-order loss of activity with T298C being inactivated from 8 to 100 times faster than wt YPK. A pH dependence of the inactivation rate constant for T298C gives a value of 8.2, consistent with the pK for a thiol. Changes in fluorescence indicate that the T298C−Mg^{2+} complex binds PEP, ADP, and both ligands together. This demonstrates that the lack of activity is not due to the loss of substrate binding but to the lack of ability to induce the proper conformational change. The mutation also induces changes in binding of FBP to all the relevant complexes. Binding of the metal and binding of PEP to the enzyme complexes are also differentially altered. Solvent isotope effects are observed for both wt and T298C. Proton inventory studies indicate that k_{cat} is affected by a proton from water in the transition state and the effects are metal ion-dependent. The results are consistent with water being the active site proton donor. Active site residue T298 is not critical for activity but plays a role in the activation of the water and affects the pK that modulates catalytic activity

Yeast pyruvate kinase (YPK,[1] EC 2.7.1.4.0) is a key regulatory enzyme in glycolysis that catalyzes the two-step reaction of phosphoryl transfer from phosphoenolpyruvate (PEP) to ADP to yield ATP followed by the protonation of enolpyruvate to form pyruvate. The reaction requires both monovalent and divalent cations, normally K^+ and Mg^{2+} or Mn^{2+}. The net reaction catalyzed by YPK is the sum of at least two partial reactions. Phosphoryl transfer from PEP to M(II)ADP occurs by an apparent S_N2 mechanism with an inversion of configuration at the phosphoryl group, to yield the enolate of pyruvate and M(II)ATP (*1*). In the second partial reaction, a proton donor at the active site stereospecifically protonates the enolate at the 2-*si* face of the double bond to form keto pyruvate (*1*−*4*) (Scheme 1). Rose and colleagues (*5*) suggested that the proton donor in pyruvate kinase is a polyprotic acid with a high pK_a that rapidly exchanges protons with solvent. Depending upon the conditions, including the divalent metal activator, as many as 3 equiv of ^3H can be incorporated into pyruvate with rabbit muscle pyruvate kinase (*6*) when the reaction is carried out in ^3H_2O. This multilabel incorporation can occur if keto−enol tautomerization is rapid relative to pyruvate departure. An initial hypothesis was that the active site Lys 240 (in the YPK numbering sequence) is responsible for enolpyruvate protonation. The recent studies of the K240M mutant of YPK by Bollenbach et al. (*7*) support the role of Lys 240 in facilitating phosphoryl transfer but not enolpyruvate protonation. Attempts to trap the proton donor (P. Loria and T. Nowak, unpublished results) using both the epoxide of PEP and Br-PEP did not result in inactivation of the enzyme. Recently published X-ray crystal structures of the yeast enzyme with bound phosphoglycolate (*8*) and of the rabbit muscle enzyme complexed with pyruvate (*9*) indicate that Thr 298 (YPK numbering) is in position to stereospecifically

† The research reported in this paper was supported in part by a research grant from the National Institutes of Health (DK 17049 to T.N.) and by the University of Notre Dame.

* To whom correspondence should be addressed: Department of Chemistry and Biochemistry, University of Notre Dame, Notre Dame, IN 46556-5670. Telephone: (574) 631-5859. Fax: (574) 631-3567. E-mail: Nowak.1@ND.edu.

[1] Abbreviations: BME, β-mercaptoethanol; CD, circular dichroism; FBP, fructose 1,6-bisphosphate; IAA, iodoacetate (Na^+ salt); LDH, L-lactate dehydrogenase; MALDI-TOF, matrix-assisted laser diode-induced time-of-flight mass spectroscopy; M(II), divalent metal cation; MES, 2-(*N*-morpholino)ethanesulfonic acid; NADH, reduced nicotinamide adenine dinucleotide; PEP, phosphoenolpyruvate; SDS−PAGE, sodium dodecyl sulfate−polyacrylamide gel electrophoresis; SIE, solvent isotope effect; T298C, yeast pyruvate kinase mutant with transformation of Thr 298 to Cys; wt, wild type; YPK, yeast pyruvate kinase.

10.1021/bi049864d CCC: $27.50
Published on Web 11/11/2004

Scheme 1[a]

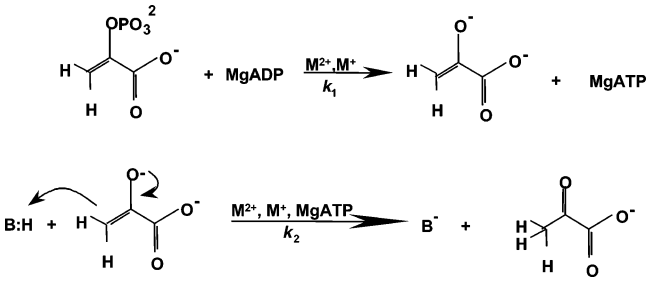

[a] Species above the arrow are required cofactors. *k* indicates net rate constants, and B:H is the putative proton donor.

protonate the enolate intermediate. Of the more than 30 pyruvate kinases sequenced to date, the amino acids at the catalytic site are 100% conserved.

The nature of the protonation step in the reaction catalyzed by pyruvate kinase has been addressed with the yeast enzyme. YPK is an allosteric enzyme with homotropic effects caused by M^{2+} and PEP. Fructose 1,6-bisphosphate (FBP) is the heterotropic activator. The FBP binding site is ~40 Å from the active site (*8*). In studies of YPK, we have constructed mutants of the putative proton donor (T298): T298S, T298A, and T298V. The first two mutant enzymes were expressed, purified, and characterized previously (*10*). T298V failed to support growth of PK-deficient yeast on glucose, which is indicative of an inactive mutant enzyme. Detailed kinetic and physical characterization of the T298S and T298A mutants indicates that T298 is not the ultimate proton donor in YPK. In k_{cat} versus pH studies, a p$K_{a,2}$ of 6.4 in the wild-type YPK is also present in the pH−rate profile of T298S and is lost with T298A (*10*). The results suggest that p$K_{a,2}$ is some function of T298. The results of these earlier studies indicate that water is the proton donor. This water molecule is in the vicinity of T298 and may be part of a proton relay at the active site. One of the water molecules in the relay is a ligand to the metal ion at the catalytic site (*10*).

In this study, the functional alcohol group on T298 is changed to a thiol group. The T298C mutant of YPK was expressed, purified, and characterized by kinetic and physical methods to further clarify the catalytic process of YPK and the nature of the proton transfer step. A primary focus of the studies with T298C is further investigation of the nature of p$K_{a,2}$ in the pH−rate profile of YPK and the chemical reactivity of the group at position 298. The results of the studies with T298C are consistent with the data obtained previously with the T298S and T298A mutants and support the hypothesis that water from a specific channel is the ultimate proton donor in YPK. The threonine or cysteine at position 298 affects the reactivity of water.

EXPERIMENTAL PROCEDURES

Materials. L-(+)-Lactate dehydrogenase from rabbit muscle was purchased from Boehringer-Mannheim. PEP, ADP, FBP, disodium NADH, glycerol, iodoacetate (sodium salt), and buffers were purchased from Sigma. Deuterium oxide (99.9%) was obtained from Cambridge Isotope Laboratories. The Altered Sites mutagenesis kit was purchased from Promega, and the mutagenic oligonucleotide was synthesized at the Biocore Facility of the Department of Chemistry and Biochemistry of the University of Notre Dame.

Site-Directed Mutagenesis. T298C was constructed and expressed using the same procedure that was used for wild-type YPK and described previously (*10*, *11*). The mutagenic oligonucleotide used for constructing the T298C point mutant is CCAACATTTGGCAAGCACAGATAACTGG, where the underlined sequence corresponds to the mutated codon that encodes the amino acid at position 298. The presence of the desired mutation was confirmed by sequence analysis of the mutated YPK gene (DNA Sequence Facility, Iowa State University, Ames, IA).

Pyruvate Kinase Purification. T298C YPK was purified as previously described (*12*) for wild-type YPK. Approximately 200 mg of enzyme was obtained from 60 g of yeast cells. For storage of T298C YPK, the concentration of β-mercaptoethanol (BME) in the storage buffer [25% glycerol, 5 mM BME, and 5 mM EDTA, in 10 mM phosphate buffer (pH 6.2) saturated in ammonium sulfate] was increased to 10 mM due to the potential susceptibility of cysteine to oxidation. The enzyme was shown to be more than 95% pure by SDS−PAGE and MALDI-TOF MS analyses.

Pyruvate Kinase Assay. Pyruvate kinase was assayed by following the decrease in absorbance at 340 nm due to NADH oxidation using the coupled assay with L-lactate dehydrogenase (LDH) (*13*). The specific activity of YPK is expressed as micromoles of NADH oxidized per minute per milligram of protein. The concentration of YPK was determined by its absorbance at 280 nm. The extinction coefficient used for YPK (ϵ_{280}) equals 0.51 M^{-1} cm^{-1}. Typical assay mixtures contained (in 1 mL) 100 mM MES (pH 6.2), 4% glycerol, 200 mM KCl, either 20 mM $MgCl_2$ or 4 mM $MnCl_2$, 5 mM ADP, 5 mM PEP, 175 μM NADH, 20 μg of LDH, and YPK (1−2 μg for the wild type or 1.5−3 μg for T298C). When present, FBP was at a concentration of 1 mM.

Steady-state reaction rates were calculated by measuring the slope of the reaction progress curve of NADH oxidation. The initial velocity data were fit to the Michaelis−Menten equation (eq 1) or to the Hill equation (eq 2), depending on which equation gave the best fit of the experimental data.

$$v/V_{max} = 1/(1 + K_m/[S]) \quad (1)$$

$$v/V_{max} = 1/[1 + (K_m/[S])^{n_H}] \quad (2)$$

Initial rates of pyruvate formation were measured as a function of variable substrate or activator concentration. The PEP concentration was varied in the absence or presence of 1 mM FBP and with Mn^{2+} or with Mg^{2+} as the divalent activator. The FBP concentration was varied in the presence of 20 mM $MgCl_2$ and 20 mM PEP. The free Mn^{2+} concentration was varied in the absence of FBP and at a constant MnADP concentration. The MnADP concentration was varied in the absence of FBP and at constant concentration of free Mn^{2+}. In all cases where the PEP concentration was kept constant, the concentration of PEP was saturating at 5 mM, unless otherwise specified. Concentrations of free Mn^{2+} and MnADP were calculated from the measured concentrations of total Mn^{2+} and total ADP using the following equation:

$$K_d = \frac{[Mn^{2+}]_{free}[ADP]_{free}}{[MnADP]} \quad (3)$$

where $[Mn^{2+}]_{free} + [MnADP] = [Mn^{2+}]_{total}$, $[ADP]_{free} + [MnADP] = [ADP]_{total}$, and $K_d = 0.125$ mM.

Effect of pH on k_{cat}. The effect of pH on the maximal velocity of the reaction catalyzed by T298C YPK was studied in the pH range of 4.9−8.8. The pH−rate profile for T298C was compared to the profile previously measured for wild-type YPK (*7*). The measurements were performed in the presence of 1 mM FBP and with Mn^{2+} (4 mM) as the divalent activator. The substrates were present at saturating concentrations of 5 mM PEP and 5 mM ADP. The buffers used were acetate (pH 4.9−5.5), MES (pH 5.0−6.8), HEPES (pH 6.5−7.7), and TAPS (pH 7.5−8.8). The buffers overlapped and had no effects on activity. The buffers were all titrated to the desired pH by using either KOH or HCl. The pH of the kinetic assay mixtures, containing all of the assay components except the coupling enzyme (LDH) and pyruvate kinase, was determined before the initiation of the reactions.

The pH−rate data measured with T298C were fit to both eqs 4 and 5, which were previously derived and described (*7*, *14*). The equation that most efficiently modeled the experimental data was chosen. $V_{max,app}$ is the observed maximal rate of a reaction at a given pH. The maximal velocity in the plateau region, V'_{max}, can be related to the maximal velocity, V_{max}, by a proportionality factor α, where $V'_{max} = \alpha V_{max}$. The value of α can be either >1 or <1, depending on whether the protons inhibit or activate the reaction rate, respectively.

$$V_{max,app} = \frac{V_{max}\left(\alpha + \frac{[H^+]}{K_B}\right)}{1 + \frac{[H^+]^2}{K_A K_B} + \frac{[H^+]}{K_B} + \frac{K_C}{[H^+]}} \quad (4)$$

$$V_{max,app} = \frac{V_{max}}{1 + \frac{[H^+]}{K_A} + \frac{K_C}{[H^+]}} \quad (5)$$

pH-Dependent Inactivation Studies with Iodoacetate. Iodoacetate (Na^+ salt) (IAA) was utilized to modify wild-type and T298C YPK over a pH range of 5.5−8.7. The buffers used were MES (pH 5.5−6.8), HEPES (pH 6.5−7.7), and TAPS (pH 7.8−8.8). YPK (0.4 mg/mL) was incubated at room temperature, in the dark, with 10 mM IAA, in 50 mM buffer, 4% glycerol, 200 mM KCl, and 0.15 mM BME. The total volume of the incubation mixture was 1 mL. As a control, an identical solution that contained no IAA was prepared for each wild-type YPK and T298C mutant. At designated time intervals (0−120 min), a 5 μL aliquot of the incubation mixture was withdrawn and assayed for PK activity by the standard PK assay containing Mn^{2+} and FBP. The 200-fold dilution of the aliquots withdrawn from the incubation mixture in the 1 mL PK assay is assumed to be sufficient to terminate the inactivation reaction by IAA. The inactivation rate constant ($k_{obs,inact}$) at each pH value was determined from the fit of the relative activity (activity of YPK in the presence of IAA relative to the activity of YPK in the absence of IAA at the same time point) at each time point to a single-exponential decay (eq 6).

$$A_{rel} = C_1 + C_2 \exp(-k_{obs,inact} t) \quad (6)$$

where A_{rel} represents the relative YPK activity and coefficients C_1 and C_2 represent the fraction of active protein and the fraction of inactive protein, respectively, upon modification with IAA. The sum of C_1 and C_2 is always 1. In the case of wild-type YPK, coefficients C_1 and C_2 equaled 0 and 1, respectively.

The log of $k_{obs,inact}$ was plotted as a function of pH and fit to eq 7 in the case of wild-type YPK or to eq 8 in the case of T298C. In eqs 7 and 8 (*15*), $[H^+]$ is the proton concentration and K_a is the dissociation constant for the group undergoing ionization. Equation 7 models the case in which a rate constant for inactivation at low pH (k_L) and a rate constant of inactivation at high pH (k_H) are defined. Equation 8 describes the model in which $k_{obs,inact}$ increases only at high pH and C represents the pH-independent rate constant.

$$\log(k_{obs,inact}) = \log\frac{k_L + k_H(K_a/[H^+])}{1 + K_a/[H^+]} \quad (7)$$

$$\log(k_{obs,inact}) = \log\frac{C}{1 + K_a/[H^+]} \quad (8)$$

At each pH value, the rate constants for inactivation by IAA measured with T298C were corrected for the background inactivation observed with the wild-type enzyme. The corrected rate constants for inactivation ($k_{cor,inact}$) were plotted against pH and fit to eq 7 to determine the K_a for the group undergoing ionization to form the carboxymethylated T298C YPK.

Steady-State Fluorescence Measurements. The experiments were performed on an SLM model 8100 spectrofluorimeter equipped with an RG630 filter in the reference channel and with an external fluorescent standard (rhodamine B in ethylene glycol, 3 g/L), and thermostated at 24 ± 1 °C. Emission spectra were recorded from 310 to 400 nm with a bandwidth of 2 nm and a scan rate of 1 nm/s. For each spectrum, four scans were averaged with an integration time of 0.1 s. Excitation of the single tryptophan, W452, was at 295 nm. Samples were in 100 mM MES buffer (pH 6.2), 200 mM KCl, and 4% glycerol. The final concentrations of all the species, not necessarily in the order of addition, were as follows: 0.06 mg/mL YPK, 20 mM $MgCl_2$ or 4 mM $MnCl_2$, 15 mM PEP (or 5 mM PEP in the presence of $MnCl_2$), 1 mM FBP (unless otherwise specified), and 5 mM ADP when present. All ligand concentrations were saturating. The fluorescence was calculated relative to the external fluorescent standard and was corrected for dilution.

The dissociation constants of the ligands to various enzyme complexes of YPK were measured by monitoring the change in fluorescence intensity at 334 nm, with excitation of W452 at 295 nm. Titrations were performed by sequentially adding 1−10 μL aliquots of a concentrated ligand solution to 900 μL of a mixture containing 100 mM MES (pH 6.2), 4% glycerol, 200 mM KCl, 0.05−0.07 mg/mL YPK, and other ligands as specified. The experimental data were processed using eqs 9 and 10 as described previously (*10*).

$$Q = \frac{Q_{max}[L]}{K_D + [L]} \quad (9)$$

$$Q = \frac{Q_{max}[L]^{n_H}}{K_D^{n_H} + [L]^{n_H}} \quad (10)$$

Circular Dichroism Spectroscopy. CD spectra of wild-type and T298C YPK were acquired on an Aviv 202SF stopped-flow circular dichroism spectrometer, at 25 ± 1 °C. The experiments were performed with protein solutions at concentrations of 0.05 mg/mL in 20 mM MES (pH 6.2), 4% glycerol, and 200 mM KCl. The concentrations of the titrated ligands are specified in the figure legends. All solutions were filtered through a 0.45 μm filter prior to the measurements. Each spectrum was recorded with a bandwidth of 1 nm and a scan rate of 1 nm/s. The scans were acquired from 280 to 200 nm. For each sample, four repetitive scans were obtained and averaged. The averaging time was 1.0 s, and the filter settling time was 0.3 s. Depending on the conditions, a scan of the buffer or a scan of the buffer and ligands is subtracted from each of the protein spectra. The observed ellipticity, θ (degrees), was converted to molar ellipticity, $[\theta]_\lambda$ (degrees per mole per square centimeter), using the following equation:

$$[\theta]_\lambda = \frac{M_{r,YPK}\theta}{10L[YPK]} \quad (11)$$

where $M_{r,YPK}$ represents the YPK subunit molecular weight (54 533 g/mol) [X-ray data for YPK from Brookhaven Protein Data Bank deposited by Jurica et al. (*8*)], L represents the quartz cell path length (0.2 cm), and [YPK] represents the concentration of either wild-type or T298C YPK (grams per milliliter). Deconvolution of the acquired CD spectra for wild-type and T298C YPK was performed as described in the Supporting Information.

Solvent Isotope Effect Studies. Solvent isotope effects (SIE) were measured with T298C YPK as described previously (*10*) and compared to the results obtained with wild-type YPK. Final concentrations for all species were 200 mM KCl, 20 mM $MgCl_2$ (or 4 mM $MnCl_2$), 5 mM ADP, and 1 mM FBP in 100 mM MES (pL 6.2). Assays (1 mL) were prepared and covered with Parafilm prior to measurements and were performed in duplicate. Solvent isotope effects on k_{cat}, $^D(k_{cat})$, and on $k_{cat}/K_{m,PEP}$, $^D(k_{cat}/K_{m,PEP})$, were determined from fits of initial velocity versus [PEP] in H_2O and D_2O to eq 1.

Proton Inventory Studies. Wild-type YPK and T298C YPK were assayed in a series of isotopically mixed water solutions ($[^1H]H_2O$ and $[^2H]H_2O$) with a deuterium molar fraction n as described previously (*10*). In each case, the initial velocities were measured at a saturating PEP concentration (5 mM PEP in the presence of $MnCl_2$ or 20 mM PEP in the presence of $MgCl_2$). Assays were performed in triplicate. The data were fit to the Gross−Butler equation (*16*) either in the linear form (eq 12) or in the nonlinear form (eq 13).

$$V_n/V_0 = 1 + n(\phi^T - 1) \quad (12)$$

$$V_n/V_0 = [1 + n(\phi^T - 1)]/[1 + n(\phi^R - 1)] \quad (13)$$

where ϕ^T and ϕ^R are the fractionation factors for the transition state and reactant state, respectively, and V_n and V_0 represent the maximal velocities observed in a mixture of isotopic water of n mole fraction of D_2O and in H_2O where $n = 0$, respectively (*16*, *17*).

RESULTS

Purification of T298C YPK. The T298C mutant YPK was purified to >95% homogeneity based on SDS−PAGE (not shown), with a yield of 20 mg of protein/L of culture. The MALDI-TOF spectrum of the purified T298C showed one peak at *m*/*z* 54 374 corresponding to the monomeric form of the mutant YPK (data not shown).

Biophysical Characterization of T298C YPK. The comparative far-UV CD spectra of the apo forms of the T298C mutant and wild-type YPK (Figure S.1, Supporting Information) indicate a slight and consistent difference in the magnitude of the molar ellipticity of the mutant YPK relative to the wild-type enzyme. The general shape of the spectra of the T298C mutant and wild-type YPK is the same over the full spectral range (200−280 nm), exhibiting double minima at 208 and 222 nm characteristic of α-helical content and a minimum at 218 nm distinctive for β-sheet structure (*18*). These results indicate that the T398C mutation does not cause any significant changes in the secondary structure and that wild-type YPK and mutant YPK are folded into a similar structure.

The intrinsic tryptophan fluorescence emission spectrum of both the apo T298C mutant and apo wild-type YPK (recorded between 310 and 400 nm) (Figure S.2, Supporting Information) exhibits a tryptophan emission maximum at approximately 334 nm. Both spectra are very similar, indicating that the environment surrounding tryptophan 452 has not been disrupted by the T298C mutation relative to wild-type YPK.

Steady-State Kinetics. The results of the kinetic experiments performed with T298C are compared to the parameters measured with wild-type YPK and are summarized in Table 1. The T298C mutant is not kinetically active with Mg^{2+} unless the heterotropic activator FBP is present (Table 1). T298C behaves kinetically in a manner similar to that of wild-type YPK with Mn^{2+} as the divalent activator. The k_{cat} measured with T298C is approximately 20% of the k_{cat} determined with wild-type YPK under the same conditions (Table 1). The divalent metal specificity with T298C is the same as for wild-type YPK ($Mg^{2+} > Mn^{2+}$) in the presence of FBP, based on k_{cat} values.

The K_m for the substrate PEP ($K_{m,PEP}$) is both divalent metal- and FBP-dependent with T298C as it is with wild-type YPK. With Mg^{2+}-activated T298C in the presence of FBP, there is a 14-fold increase in the $K_{m,PEP}$ compared to that for the Mg^{2+}- and FBP-activated wild-type YPK (Table 1). Kinetic measurements with T298C were performed at an increased concentration of total Mg^{2+} (20 mM) relative to that with the wild type (15 mM $MgCl_2$) and at 5 mM ADP and in the presence of 1 mM FBP. When the concentration of MgADP is 10 mM and $[Mg^{2+}]_{free} = 5$ mM in the presence of 1 mM FBP, or in the presence of 20 mM $MgCl_2$, 5 mM ADP, and 2 mM FBP, the $K_{m,PEP}$ measured with T298C did not change. The value of $k_{cat}/K_{m,PEP}$ measured in the presence of Mg^{2+} and FBP is decreased by 2 orders of magnitude for T298C relative to that for wild-type YPK.

Table 1: Steady-State Kinetic Parameters for Wild-Type and T298C YPK[a]

divalent activator	ligand	FBP	YPK	k_{cat} (s^{-1})	K_m (μM)	$k_{cat}/K_{m,PEP}$ (M^{-1} s^{-1})	n_H
Mg^{2+}	PEP	no	wild-type[b]	232 ± 5	1180 ± 220	(2.0 ± 0.5) × 10^5	2.80 ± 0.10
	PEP	no	T298C	<**0.1**	nd[c]	nd[c]	nd[c]
	PEP	yes	wild-type[b]	226 ± 11	310 ± 5	(7.3 ± 0.5) × 10^5	1.0
	PEP	yes	T298C[d]	41.3 ± 0.8	4430 ± 220	(9.3 ± 0.5) × 10^3	1.0
	FBP		wild-type[e]	236 ± 4	13.0 ± 0.1		**1.0**
	FBP		T298C[f]	33.0 ± 0.2	144 ± 0		**2.60 ± 0.04**
Mn^{2+}	PEP	no	wild-type[b]	58.4 ± 0.9	45 ± 1	(1.3 ± 0.1) × 10^6	2.50 ± 0.10
	PEP	no	T298C	12.2 ± 0.2	242 ± 7	(5.0 ± 0.1) × 10^4	1.50 ± 0.06
	PEP	yes	wild-type[b]	66.0 ± 1.8	21 ± 3	(3.1 ± 0.6) × 10^6	1.0
	PEP	yes	T298C	13.9 ± 0.2	66 ± 4	(2.1 ± 0.3) × 10^5	1.0

[a] Steady-state kinetic parameters were measured as described in Experimental Procedures. When the PEP concentration was varied, the concentrations of all other species were saturating and were as follows: 4 mM $MnCl_2$ or 15 mM $MgCl_2$, 5 mM ADP, 1 mM FBP (when present) and 200 mM KCl in 100 mM MES (pH 6.2), and 4% glycerol. Kinetic constants were obtained from fits of either eq 1 or 2 to initial velocity data as a function of variable ligand concentration. [b] Taken from Bollenbach et al. (*7*). [c] Not determined due to a lack of catalytic activity. [d] The total $MgCl_2$ concentration was 20 mM. [e] Taken from Bollenbach and Nowak (*19*). [f] [PEP] = 20 mM. [$MgCl_2$] = 20 mM. [ADP] = 5 mM.

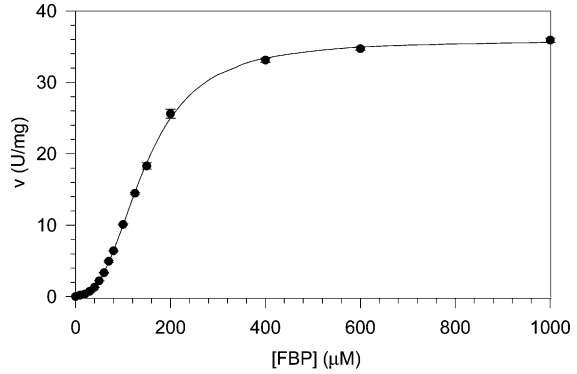

FIGURE 1: Steady-state velocity response of Mg^{2+}-activated T298C YPK as a function of FBP concentration. The velocity response as a function of FBP concentration is sigmoidal and is best fit to eq 2. Error bars in the data represent deviations from replicate determinations. The parameters giving the best fit are listed in Table 1. The experiment was carried out in 100 mM MES (pH 6.2), 4% glycerol, 200 mM KCl, 20 mM $MgCl_2$, 5 mM ADP, and 20 mM PEP. All concentrations were saturating. At each FBP concentration, the measured initial rates were corrected for the residual initial rate of pyruvate formation at zero FBP concentration (<0.1 unit/mg).

With Mg^{2+}-activated T298C, there is a 10-fold increase in the K_m for FBP (144 ± 1 μM) relative to that of wild-type YPK (13.0 ± 0.1 μM) (Table 1). At saturating concentrations of PEP, Mg^{2+}, and MgADP, the kinetic response to a variable FBP concentration changes from hyperbolic in the wild type (n_H = 1.0) to sigmoidal in T298C (n_H = 2.6) (T298C is inactive when [FBP] = 0) (Figure 1). The thermodynamically determined parameters for FBP binding to the YPK−Mg^{2+}−PEP complex are as follows: $K_{d,FBP}$ = 7.3 ± 0.6 μM and n_H = 1.3 ± 0.1 for the wild type and $K_{d,FBP}$ = 78 ± 2 μM and n_H = 1.9 ± 0.1 for T298C YPK (vide infra, Table 5). With both wild-type and T298C YPK, the $K_{m,FBP}$ is similar to the $K_{d,FBP}$ measured by fluorescence. FBP is in apparent thermodynamic equilibrium with YPK during steady-state turnover. FBP binds to the YPK−Mg^{2+}−PEP complex with positive cooperativity with both wild-type and T298C YPK. Thus, MgADP must influence the homotropic cooperativity of FBP binding to wild-type (*19*) and T298C YPK. Kinetically, in the fully ligated complex, the homotropic interaction of FBP is heterotropically abolished by MgADP in wild-type YPK and is enhanced in T298C YPK.

With Mn^{2+}-activated T298C, the $K_{m,PEP}$ increases 5- and 3-fold relative to that of wild-type YPK in the absence and presence of FBP, respectively (Table 1). The second-order rate constant, $k_{cat}/K_{m,PEP}$, is decreased by 2 orders of magnitude and 1 order of magnitude relative to that of wild-type YPK in the absence and presence of FBP, respectively. The kinetic response of T298C to a variable PEP concentration in the absence of FBP is sigmoidal, as with wild-type YPK, but to a lesser extent ($n_{H,PEP}$ = 1.5 vs $n_{H,PEP}$ = 2.5).

Table 2: Steady-State Kinetic Parameters for Mn^{2+}-Activated Wild-Type and T298C YPK[a]

ligand	FBP	YPK	K_m (μM)	n_H
free Mn^{2+}	no	wild-type[b]	15.0 ± 0.1	2.0 ± 0.3
	no	T298C	49.7 ± 1.6	2.6 ± 0.2
MnADP	no	wild-type[c]	250 ± 20	1.0
	no	T298C	409 ± 16	1.0

[a] Nonvaried substrates were held saturating: 5 mM PEP, 1 mM free Mn, and 2 mM MnADP. [b] Taken from Mesecar and Nowak (*12*). [c] Taken from Bollenbach (*11*).

The kinetic constants for free Mn^{2+} and MnADP in the absence of FBP measured with T298C are summarized in Table 2. The K_m for free Mn^{2+} is increased 3-fold relative to that of wild-type YPK, but is still in the micromolar range (Table 2). The homotropic cooperativity with free Mn^{2+} for T298C is similar to that of wild-type YPK (n_H = 2.0 vs n_H = 2.6). The T298C mutation causes a 2-fold increase in the K_m for MnADP (Table 2). The kinetic response with MnADP as a variable substrate is hyperbolic in both wild-type and T298C YPK. These kinetic constants with Mg^{2+} could not be measured with T298C due to lack of kinetic activity in the absence of FBP.

Effect of pH on Catalysis by Wild-Type and T298C YPK. The possible relevance of T298 to an ionization that affects catalysis was addressed by measuring pH−rate profiles. Figure 2 shows the pH−rate profile for T298C activated by Mn^{2+} and by FBP. For the purposes of comparison, the pH−rate profiles for wild-type YPK and T298A that are activated by Mn^{2+} and by FBP (*10*) are also presented. The same profiles are obtained for the Mg^{2+}-activated enzymes (*10*). The pH−rate profile for T298C shows a slope of 2 in the acidic region in contrast to the pH−rate profiles of wild-type and T298A YPK that have a slope of 1. These results are consistent with the ionization of two groups in T298C and the ionization of one group with the wild type and with T298A, respectively, in the acidic pH region. The pH−rate data for T298C were fit to three models: (1) eq 4, which

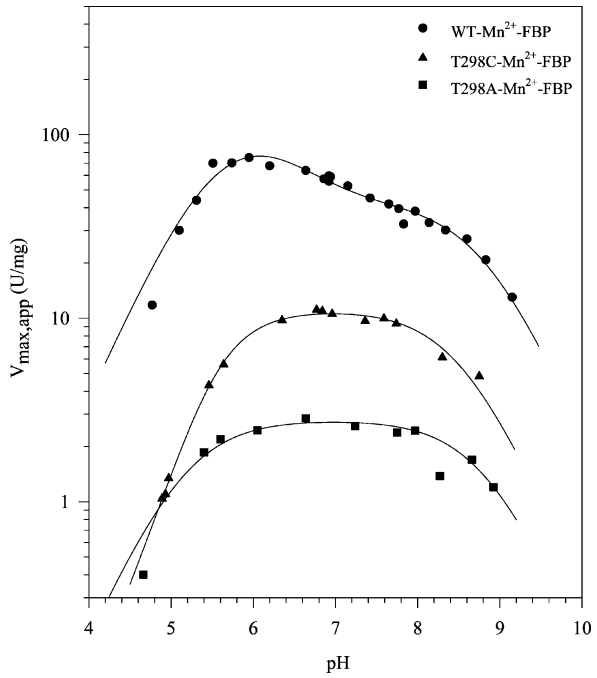

FIGURE 2: Effect of pH on $V_{max,app}$ for wild-type, T298C, and T298A YPK. The effect of pH on $V_{max,app}$ for Mn^{2+}-activated wild-type (●) (*7*), T298C (▲), and T298A (■) (*10*) is shown. $V_{max,app}$ with T298C was measured in the presence of saturating concentrations of PEP (5 mM) and of all ligands (4 mM $MnCl_2$, 5 mM ADP, 1 mM FBP, and 200 mM KCl). The curves represent the best fit to eq 4 for wild-type YPK, to eq 4 (where $pK_A = 5.5$) for T298C YPK, and to eq 5 for T298A YPK. The pK_a values giving the best-fit parameters are listed in Table 3.

Table 3: pH Effects on k_{cat} for Wild-Type, T298C, and T298A YPK[a]

YPK	pK_A	pK_B	pK_C
wild-type[b]	5.5 ± 0.1	6.4 ± 0.3	8.8 ± 0.2
T298C	5.5 ± 0.1	5.5 ± 0.2	8.5 ± 0.1
T298A[c]	5.2 ± 0.1		8.8 ± 0.1

[a] The effect of pH on k_{cat} with T298C was measured as described in Experimental Procedures at saturating concentrations of PEP and all ligands. [b] Taken from Bollenbach et al. (*7*). [c] Taken from Susan-Resiga and Nowak (*10*).

describes the ionization of three groups; (2) eq 4 in which the value for pK_A was imposed as 5.5, the same value as for wild-type YPK; and (3) eq 5, which describes the ionization of only two groups. The parameters obtained from the fit to each model and the statistical summary of each fit are listed in Table S.1 of the Supporting Information. The $K_{m,PEP}$ values measured for the Mn^{2+}- and FBP-activated wild type and mutants T298S and T298A were invariant over the pH range that was studied (*20*), allowing the calculation of pK_a values for "E_{free}". The assumption is made that T298C YPK behaves similarly.

On the basis of the statistical analysis (Table S.1, Supporting Information) and the slope of 2 in the acidic range of the pH−rate profile (Figure 2), the second model, defined by eq 4 in which $pK_A = 5.5$, best describes the pH−rate data measured with T298C YPK. Table 3 lists the pK_a values that result from the best fit of the pH−rate data. Mutation of the functional group T298 from a hydroxyl in wild-type YPK to a thiol in T298C results in an acidic shift of pK_B from 6.4 to 5.5 (Table 3). When the functional group is removed in T298A YPK, pK_B is lost (*10*).

pH-Dependent Inactivation Studies with Iodoacetate. Iodoacetate (IAA) reacts with good nucleophiles, and cysteine is potentially the most powerful nucleophile in a protein. Wild-type YPK has no cysteine located in the active site (*8*). Mutation of Thr 298 to Cys introduces a potentially new nucleophile into the active site of YPK. The possibility of the unique reactivity of cysteine in T298C YPK was used to determine the nature of the second pK_a (pK_B) in the pH−rate profile. IAA inactivation studies were performed with wild-type YPK and T298C as a function of pH.

A plot of the observed rate constants for IAA inactivation of wild-type YPK with respect to pH is shown in Figure 3A. For T298C, the observed rate constant for inactivation by IAA at each pH was corrected for the background inactivation measured with wild-type YPK. The rate constant for IAA inactivation of T298C is 10−125-fold greater than that for wild-type YPK (Table 4). A plot of the corrected rate constants for inactivation ($k_{corr,inact}$) against pH is presented in Figure 3B. A fit to the uncorrected rate constants gives nearly identical results. The best fit to eq 8 of the IAA inactivation data with wild-type YPK (Figure 3A) yields a pK_a value of 8.71 ± 0.07 with a pH-independent value for the rate constant of inactivation of (1.15 ± 0.15) × 10^{-3} min^{-1}. With T298C YPK, the data for inactivation by IAA are best fit by eq 7 (Figure 3B), yielding a pK_a value of 8.20 ± 0.12 with a limit to the observed reaction rate constant of 0.006 ± 0.001 min^{-1} at low pH increasing to 1.03 ± 0.21 min^{-1} at high pH. The S-carboxymethylated T298C YPK remains 10−15% active (see C_1 values in Table 4).

Steady-State Fluorescence Titrations. Yeast pyruvate kinase is a homotetramer with overall D_2 symmetry. YPK contains a single tryptophan residue per monomer, Trp 452, that is situated near the dimer−dimer interface. Trp 452 provides an internal fluorescent probe, since its intrinsic fluorescence is sensitive to binding of ligands at both the active site and the allosteric site on YPK (*21*−*23*).

Steady-state fluorescence measurements were performed to determine the effect of mutation on binding of substrates to the enzyme. The results of emission scans of T298C sequentially titrated with Mg^{2+}, PEP, and FBP and with FBP, Mg^{2+}, and PEP are shown in Figure S.3A,B of the Supporting Information. In both cases, the quaternary enzyme−ligand complex is formed and results in the same total fluorescence quenching. This indicates that the structure of the enzyme surrounding Trp 452 is the same regardless of the order of addition of FBP for formation of the quaternary enzyme−ligand complex. The results are also consistent with those obtained with wild-type YPK (*23*).

The fluorescence spectra of T298C sequentially titrated with Mg^{2+}, ADP, and PEP and with PEP, Mg^{2+}, and ADP are shown in Figure 4A,B. For reference, the results of emission scans of wild-type YPK sequentially titrated with Mg^{2+} and ADP are displayed in Figure 5. The formation of the YPK−Mg^{2+}−ADP−PEP or YPK−PEP−Mg^{2+}−ADP could not be measured with wild-type YPK because of catalytic turnover. Saturation of the T298C−Mg^{2+} complex with ADP causes a 13% quenching at 334 nm, with a concomitant 2 nm red shift (Figure 4A). This behavior is similar for the wt−Mg^{2+} complex upon saturation with ADP (Figure 5). The total fluorescence quenching upon formation of the YPK−Mg^{2+}−ADP complex is 17% with wild-type YPK and 23% with T298C YPK. This suggests that the

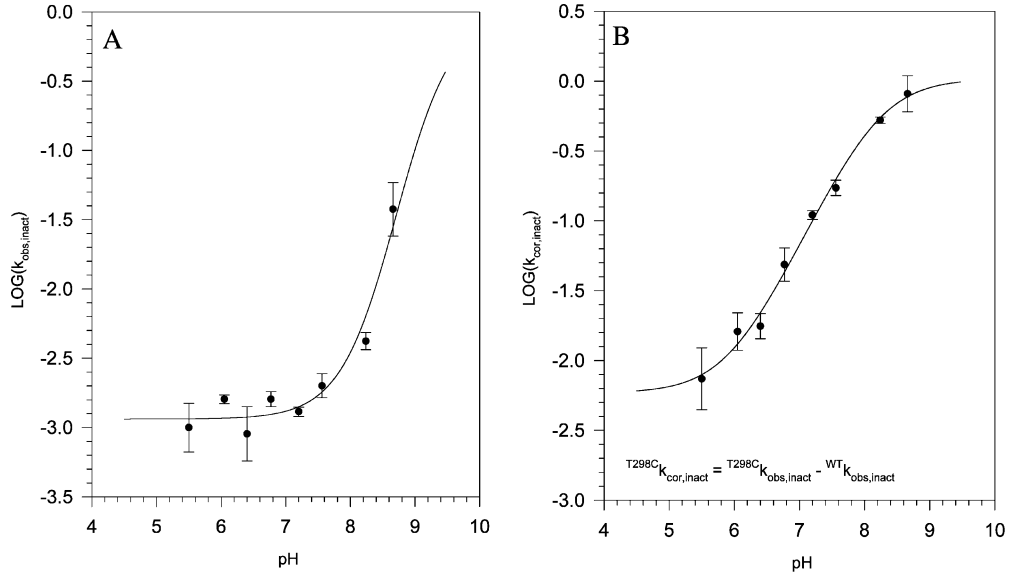

FIGURE 3: pH dependence of the rate constant for inactivation by iodoacetate of YPK. (A) Inactivation of wild-type YPK by iodoacetate. (B) Inactivation of T298C YPK by iodoacetate. YPK (0.4 mg/mL) was incubated in the presence of 10 mM IAA. Samples were withdrawn at various time periods and tested for catalytic activity. The inactivation rate constant ($k_{obs,inact}$) at each pH was determined from the fit of the relative activity to a single-exponential decay (eq 6). The log of $k_{obs,inact}$ is plotted against the pH of the incubation mixture. Error bars represent the error in the fit of the time-dependent inactivation data at each pH to eq 6. The curves through the data are from a least-squares fit of the data to eq 8, for wild-type YPK, and to eq 7, for T298C YPK. The fit generates a pK_a of 8.7 ± 0.1 with wild-type YPK and a pK_a of 8.2 ± 0.1 with T298C YPK.

Table 4: Summary of the Best-Fit Parameters for Inactivation by Iodoacetate of Wild-Type and T298C YPK[a]

YPK	pH	$k_{obs,inact}$ (min^{-1})	C_1[b]	C_2[c]
wild-type	5.50	$(1.0 \pm 0.2) \times 10^{-3}$	0	1
	6.05	$(1.6 \pm 0.1) \times 10^{-3}$	0	1
	6.40	$(0.9 \pm 0.2) \times 10^{-3}$	0	1
	6.77	$(1.6 \pm 0.1) \times 10^{-3}$	0	1
	7.20	$(1.3 \pm 0.1) \times 10^{-3}$	0	1
	7.56	$(2.0 \pm 0.2) \times 10^{-3}$	0	1
	8.24	$(4.2 \pm 0.3) \times 10^{-3}$	0	1
	8.66	$(37.6 \pm 8.2) \times 10^{-3}$	0	1
T298C	5.50	$(8.4 \pm 2.1) \times 10^{-3}$	0.12 ± 0.08	0.89 ± 0.12
	6.05	$(17.7 \pm 2.7) \times 10^{-3}$	0.31 ± 0.04	0.69 ± 0.04
	6.40	$(18.5 \pm 1.9) \times 10^{-3}$	0.19 ± 0.03	0.80 ± 0.03
	6.77	$(50.2 \pm 6.8) \times 10^{-3}$	0.19 ± 0.02	0.77 ± 0.04
	7.20	$(111 \pm 4) \times 10^{-3}$	0.14 ± 0.01	0.86 ± 0.01
	7.56	$(174 \pm 11) \times 10^{-3}$	0.13 ± 0.01	0.87 ± 0.02
	8.24	$(529 \pm 14) \times 10^{-3}$	0.10 ± 0.002	0.90 ± 0.01
	8.66	$(850 \pm 120) \times 10^{-3}$	0.10 ± 0.004	0.90 ± 0.02

[a] The rate constant for inactivation ($k_{obs,inact}$) at each pH was determined from a fit of the relative activity at each time point to eq 6. In the case of wild-type YPK, the inactivation data were best-fit to a simplified form of eq 6 [$A_{rel} = \exp(-k_{obs,inact}t)$ corresponding to $C_1 = 0$ and $C_2 = 1$]. [b] C_1 from eq 6 represents the fraction of active protein upon modification with iodoacetate. [c] C_2 from eq 6 represents the fraction of inactive protein upon modification with iodoacetate.

environment surrounding Trp 452 in the YPK−Mg^{2+}−ADP complex is slightly different in wild type and in T298C YPK. PEP binding to the T298C−Mg^{2+}−ADP complex results in an additional 20% quenching with no further change in emission maximum (Figure 4A). The total fluorescence quenching upon formation of the T298C−Mg^{2+}−ADP−PEP complex is 43%.

When apo T298C is saturated with PEP, a 25% quenching occurs at 334 nm (Figure 4B). Formation of the T298C−PEP−Mg^{2+} complex causes an additional small 5% quenching. Binding of ADP to the latter complex results in an additional 5% quenching and a 2 nm red shift. The total fluorescence quenching upon formation of the T298C−PEP−Mg^{2+}−ADP complex is 35%. The total fluorescence quenching upon formation of the quaternary enzyme−ligand complex is different, depending on the order of addition of ligands Mg^{2+}, ADP, and PEP. The results presented in Figure 4 and Figure S.3 indicate that substrates MgADP and PEP both bind to the enzyme−Mg^{2+} complex of T298C, inducing conformational changes, although no catalytic activity by T298C is observed with Mg^{2+} as the activator and in the absence of FBP.

Similar fluorescence emission spectra for T298C were measured in the presence of Mn^{2+}. The results are detailed in Figure S.4A,B of the Supporting Information. The trends in the fluorescence spectral changes that are observed with T298C and its Mn^{2+} complexes are the same as the changes observed with wild-type YPK and its Mn^{2+} complexes (*21*).

Ligand Binding by Steady-State Fluorescence. The binding of PEP, divalent metal, MgADP, and FBP to various complexes of T298C YPK was assessed by steady-state fluorescence titrations. An example of a binding isotherm is presented in Figure S.5. The binding data were fit to either a hyperbolic model (eq 9) or a sigmoidal model (eq 10). The best-fit parameters for the apparent dissociation constant (K_D), maximal fluorescence quenching (Q_{max}), and Hill coefficient (n_H) are listed in Tables 5 and 6.

Interaction of PEP with T298C Complexes. PEP binding to the apo form of both wild-type and T298C YPK is hyperbolic ($n_H = 1$, Table 5). This suggests that the binding of PEP to the apoenzyme does not involve communication among the four PEP binding sites on the tetramer. The binding of PEP to the T298C−Mg^{2+} complex has an apparent dissociation constant of 1294 μM, a 2-fold decrease relative to that of wild-type YPK (Table 5). The enzyme-bound Mg^{2+} has an antagonistic effect on the binding of PEP to both wild-type and T298C YPK. In both cases, the $K_{D,PEP}$ for the YPK−Mg^{2+} complex is greater than the $K_{D,PEP}$ for apo YPK. The measurement of the level of binding of PEP

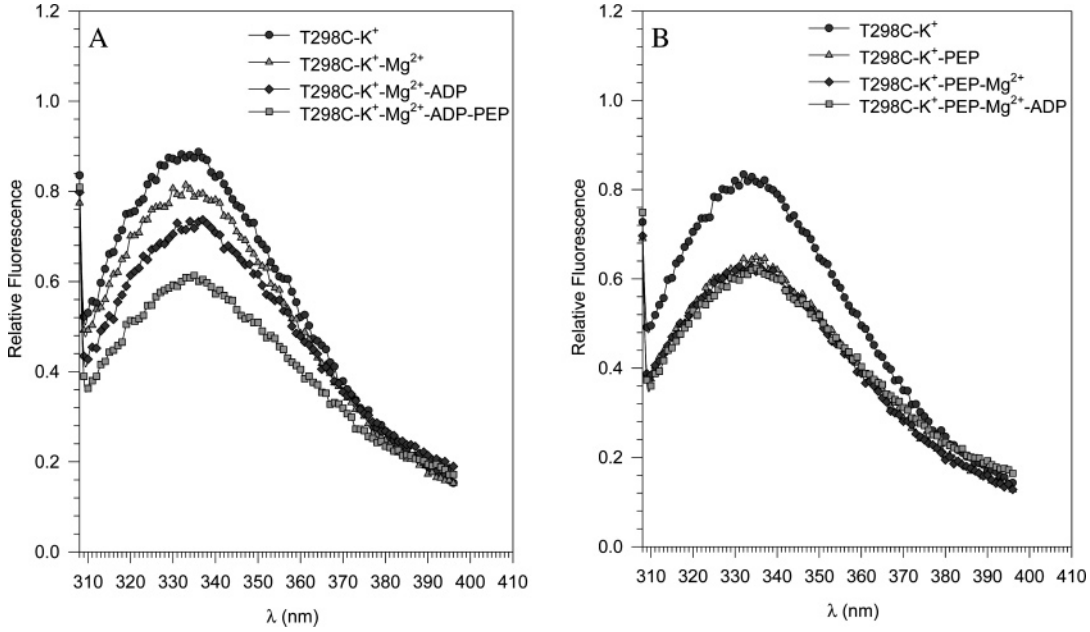

FIGURE 4: Fluorescence spectra of T298C YPK and its complexes with Mg^{2+}, PEP, and ADP. (A) Formation of the T298C−Mg^{2+}−ADP−PEP complex by sequential titration. (B) Formation of the T298C−PEP−Mg^{2+}−ADP complex by sequential titration. Trp 452 was excited at 295 nm, and emission spectra were monitored from 310 to 400 nm. The key for the symbols designating each enzyme complex is given in the inset. Final concentrations for all species were as follows: 0.06 mg/mL YPK, 200 mM KCl, 20 mM $MgCl_2$, 5 mM ADP, and 15 mM PEP (A) or 20 mM PEP (B). All ligand concentrations were saturating. The relative fluorescence is calculated with respect to an external fluorescence standard and has been corrected for dilution.

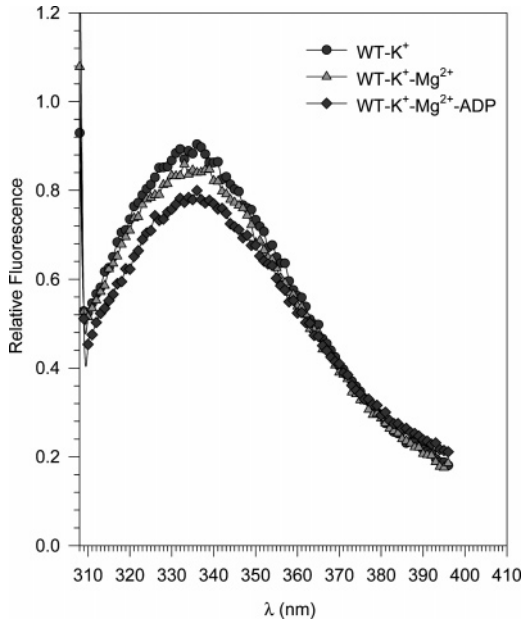

FIGURE 5: Fluorescence emission spectra of wild-type YPK and of its complexes with Mg^{2+} and ADP. Trp 452 was excited at 295 nm, and emission spectra were monitored from 310 to 400 nm. The key for the symbols designating each enzyme complex is given in the inset. Final concentrations for all species were as follows: 0.06 mg/mL YPK, 200 mM KCl, 20 mM $MgCl_2$, and 5 mM ADP. All ligand concentrations were saturating. The relative fluorescence is calculated with respect to an external fluorescence standard and has been corrected for dilution.

to the T298C−Mg^{2+}−MgADP complex could be done by steady-state fluorescence because of the lack of catalytic turnover by T298C with Mg^{2+} and in the absence of FBP (Table 1). PEP binds to the T298C−Mg^{2+}−MgADP complex in a hyperbolic manner and with a K_D of 1800 μM (Table 5). MgADP further antagonizes PEP binding to T298C.

The K_D for the interaction of PEP with the YPK−Mn^{2+} complex is significantly higher with T298C (235 μM) than with wild-type YPK (9 μM) (Table 5). While this interaction is hyperbolic with T298C ($n_H = 1$), PEP binding to the wild type−Mn^{2+} complex shows a high degree of homotropic cooperativity ($n_H = 2$). Binding of PEP to complexes of T298C in the presence of saturating FBP could not be assessed by steady-state fluorescence since very little if any change in the fluorescence intensity occurs upon addition of PEP to the T298C−FBP or T298C−Mg^{2+}(or Mn^{2+})−FBP complex. This was also observed with wild-type YPK (*21*, *23*).

Interaction of Mg^{2+} with T298C Complexes. The fluorescence response of apo T298C to Mg^{2+} concentrations is hyperbolic. The affinity of the apoenzyme for Mg^{2+} is 2-fold tighter with T298C (5730 μM) than with wild-type YPK (11 900 μM) (Table 5). The binding isotherm for the interaction of Mg^{2+} with the YPK−PEP complex is hyperbolic with T298C ($n_H = 1$) and sigmoidal with wild-type YPK ($n_H = 1.9$) (Table 5). The apparent affinity of the YPK−PEP complex for Mg^{2+} is similar for T298C (3570 μM) and wild-type YPK (4040 μM).

Interaction of Mn^{2+} with T298C Complexes. The apparent dissociation constant for Mn^{2+} binding to apo T298C (1900 μM) is 3.8-fold lower than that for binding to apo wild-type YPK (7160 μM) (Table 6). There is a small degree of negative homotropic cooperativity in the binding of Mn^{2+} to T298C ($n_H = 0.7$). The interaction between Mn^{2+} and apo wild-type YPK is hyperbolic. The binding of Mn^{2+} to the YPK−PEP complex is sigmoidal with both T298C ($n_H = 2.2$) and wild-type YPK ($n_H = 1.7$) (Table 6). The apparent affinity of the T298C−PEP complex for Mn^{2+} (128 μM) is 13-fold weaker than the affinity of the wild-type YPK−PEP complex for Mn^{2+} (10 μM). The binding of PEP to apo wild-type YPK heterotropically induces homotropic cooperativity

Table 5: Ligand Binding to Wild-Type and T298C Yeast Pyruvate Kinase Complexes by Steady-State Fluorescence (Mg^{2+} as the divalent metal)[a]

		wild type[b]				T298C			
	ligand	Q_{max} (%)	K_D (μM)	n_H	ΔG (kcal/mol)	Q_{max} (%)	K_D (μM)	n_H	ΔG (kcal/mol)
YPK	PEP	20.1 ± 0.4	638 ± 53	1	-4.33 ± 0.05	25.5 ± 0.3	488 ± 21	1	-4.48 ± 0.02
YPK$-Mg^{2+}$	PEP	34.7 ± 0.9	2810 ± 170	1	-3.45 ± 0.03	28.4 ± 0.5	1290 ± 70	1	-3.91 ± 0.03
YPK$-Mg^{2+}-$MgADP	PEP	nd[c]	nd[c]	nd[c]	nd[c]	20.1 ± 0.2	1800 ± 60	1	-3.72 ± 0.02
YPK	Mg^{2+}	3.5 ± 0.2	11900 ± 1800	nd[c]	-2.61 ± 0.09	9.6 ± 0.3	5730 ± 600	1	-3.04 ± 0.06
YPK$-$PEP	Mg^{2+}	14.3 ± 0.4	4040 ± 210	**1.85 ± 0.14**	-3.24 ± 0.03	5.4 ± 0.2	3570 ± 460	**1**	-3.31 ± 0.03
YPK$-Mg^{2+}$	MgADP	13.6 ± 0.7	634 ± 105	1	-4.33 ± 0.09	13.0 ± 0.7	676 ± 103	1	-4.29 ± 0.08
YPK$-Mg^{2+}-$PEP	MgADP	nd[c]	nd[c]	nd[c]	nd[c]	5.3 ± 0.4	768 ± 155	1	-4.22 ± 0.11
YPK	FBP	52.0 ± 0.8	321 ± 7	2.38 ± 0.09	-4.73 ± 0.02	54.2 ± 0.2	25.5 ± 0.2	1.60 ± 0.02	-6.22 ± 0.01
YPK$-$PEP	FBP	36.0 ± 1.0	217 ± 6	2.27 ± 0.09	-4.97 ± 0.01	38.4 ± 0.8	169 ± 5	1.78 ± 0.09	-5.11 ± 0.02
YPK$-Mg^{2+}$	FBP	51.4 ± 0.5	145 ± 3	3.09 ± 0.16	-5.20 ± 0.01	52.4 ± 0.2	15 ± 0.2	1.79 ± 0.03	-6.53 ± 0.01
YPK$-Mg^{2+}-$PEP	FBP	26.6 ± 1.1	7.3 ± 0.6	1.30 ± 0.08	-7.01 ± 0.05	37.2 ± 0.5	78 ± 2	1.90 ± 0.09	-5.56 ± 0.02

[a] The parameters were determined by steady-state fluorescence titrations as described in Experimental Procedures. The concentration of YPK is 0.06 mg/mL in the presence of 200 mM KCl and 4% glycerol. Final concentrations of the other ligands were as follows: 20 mM $MgCl_2$, 10 mM PEP, 1 mM FBP, and 5 mM ADP, when indicated. All ligand concentrations were saturating. For MgADP binding studies, increments of a 50.6 mM MgADP solution ($[Mg]_{free} = 1.3$ mM) were titrated into the mixture containing the YPK complex. [b] From Bollenbach and Nowak (*23*). [c] Not determined.

Table 6: Ligand Binding to Wild-Type and T298C Yeast Pyruvate Kinase Complexes by Steady-State Fluorescence (Mn^{2+} as the divalent metal)[a]

		wild type[b]				T298C			
	ligand	Q_{max} (%)	K_D (μM)	n_H	ΔG (kcal/mol)	Q_{max} (%)	K_D (μM)	n_H	ΔG (kcal/mol)
YPK	PEP	20.1 ± 0.4	638 ± 53	1	-4.33 ± 0.05	25.5 ± 0.3	488 ± 21	1	-4.48 ± 0.02
YPK$-Mn^{2+}$	PEP	34.0 ± 2.0	9 ± 0.3	**2.00 ± 0.10**	-6.83 ± 0.02	39.7 ± 0.3	235 ± 6	**1**	-4.91 ± 0.01
YPK	Mn^{2+}	9.3 ± 0.5	7160 ± 930	**1**	-2.90 ± 0.07	21.2 ± 0.2	1900 ± 460	**0.70 ± 0.07**	-3.68 ± 0.12
YPK$-$PEP	Mn^{2+}	22.2 ± 0.3	10.0 ± 0.2	2.20 ± 0.10	-6.77 ± 0.01	26.0 ± 0.6	128 ± 6	1.70 ± 0.11	-5.27 ± 0.03
YPK	FBP	52.0 ± 0.8	321 ± 7	2.38 ± 0.09	-4.73 ± 0.02	54.2 ± 0.2	25.5 ± 0.2	1.60 ± 0.02	-6.22 ± 0.01
YPK$-$PEP	FBP	36.0 ± 1.0	217 ± 6	2.27 ± 0.09	-4.97 ± 0.01	38.4 ± 0.8	169 ± 5	1.78 ± 0.09	-5.11 ± 0.02
YPK$-Mn^{2+}$	FBP	47.7 ± 0.1	50.4 ± 0.9	2.20 ± 0.10	-5.81 ± 0.01	46.3 ± 0.6	14.1 ± 0.4	1.55 ± 0.06	-6.57 ± 0.02
YPK$-Mn^{2+}-$PEP	FBP	19.2 ± 0.3	3.1 ± 0.1	1.30 ± 0.08	-7.46 ± 0.02	22.7 ± 0.2[c]	8.3 ± 0.2	1.39 ± 0.05	-6.88 ± 0.01

[a] The parameters were determined by steady-state fluorescence titrations as described in Experimental Procedures. The concentration of YPK is 0.06 mg/mL in the presence of 200 mM KCl and 4% glycerol. Final concentrations of the other ligands were as follows: 20 mM $MnCl_2$ and 10 mM PEP, unless otherwise specified. All ligand concentrations were saturating. [b] From Mesecar and Nowak (*21*). [c] Final concentrations of ligands were as follows: 4 mM $MnCl_2$ and 5 mM PEP.

of Mn^{2+} binding. In T298C, binding of PEP to the apoenzyme changes the homotropic cooperativity of Mn^{2+} binding from negative to positive.

Interaction of FBP with T298C Complexes. The binding of FBP to apo T298C is 13-fold tighter than the interaction between FBP and apo wild-type YPK (Table 5). The degree of positive homotropic cooperativity in FBP binding is significantly lower with T298C ($n_H = 1.6$) than with wild-type YPK ($n_H = 2.4$). The cooperative binding of FBP to YPK remains unchanged in the presence of saturating PEP with both T298C and wild-type YPK (Table 5). With T298C, PEP causes a 7-fold increase in the $K_{D,FBP}$, from 25 to 169 μM, suggesting that PEP and FBP have an antagonistic binding relationship in the absence of the divalent metal. With wild-type YPK, PEP and FBP show a weak and positive coupling in the absence of divalent metal. The binding of FBP to the YPK$-Mg^{2+}$ complex is 10-fold tighter with T298C than with wild-type YPK (Table 5). The degree of homotropic cooperativity is significantly less with T298C ($n_H = 1.8$) than with wild-type YPK ($n_H = 3.1$). The presence of Mg^{2+} differentially affects the binding of FBP to the E$-Mg^{2+}$ and E$-Mg^{2+}-$PEP complexes of wild-type and T298C YPK (Table 5). The Hill coefficient for FBP binding remains unchanged with T298C ($n_H = 1.9$), while with wild-type YPK, the Hill coefficient for FBP binding decreases to 1.3. The interactions between FBP and the YPK$-Mn^{2+}$ and YPK$-Mn^{2+}-$PEP complexes are qualitatively similar to the effect by Mg^{2+} except for binding to the YPK$-Mn^{2+}-$PEP complex. Binding of FBP to the ternary YPK$-M^{2+}-$PEP complex is enhanced in the presence of Mn^{2+} and weakened in the presence of Mg^{2+} (Table 6). With the YPK$-Mn^{2+}$ complex, the degree of homotropic cooperativity is significantly lower with T298C ($n_H = 1.6$) than with wild-type YPK ($n_H = 2.2$) (Table 6).

Interaction of MgADP with T298C Complexes. The affinity of the YPK$-$Mg complex for MgADP is similar for T298C (680 μM) and wild-type YPK (630 μM); both binding isotherms fit to a rectangular hyperbola ($n_H = 1$) (Table 5). The measurable change in fluorescence intensity upon MgADP binding to the T298C$-Mg^{2+}$ complex indicates that the substrate MgADP binds to the binary complex in the same manner as MgADP binds to wild-type YPK. PEP also binds to the T298C$-Mg^{2+}-$ADP complex (vide supra and Table 5). The lack of catalytic activity of T298C with Mg^{2+} and in the absence of FBP is not due the elimination of substrate binding. The apparent dissociation constant for MgADP binding to the T298C$-Mg^{2+}-$PEP complex (770 μM) is slightly increased relative to that for binding to the T298C$-Mg^{2+}$ (680 μM) complex (Table 5).

In summary, the T298C mutation has affected the interaction of FBP with all enzyme complexes and the interaction of PEP and Mn^{2+} with their respective binary enzyme

Table 7: Secondary Structure Elements Calculated for the CD Spectra of Wild-Type and T298C YPK[a]

	wild type						T298C					
	α-helix (%)	antiparallel (%)	parallel (%)	β-turn (%)	random coil (%)	total (%)	α-helix (%)	antiparallel (%)	parallel (%)	β-turn (%)	random coil (%)	total (%)
apo YPK	13.7	25.2	5.6	19.2	34.9	98.6	22.0	18.3	5.7	18.7	33.9	98.6
YPK−Mg^{2+}	**9.3**	**31.5**	5.5	19.4	35.4	101.1	**25.6**	**15.7**	5.7	17.9	32.3	97.1
YPK−Mg^{2+}−PEP	**15.8**	**22.8**	5.6	18.8	34.2	97.2	**25.5**	**16.0**	5.7	18.3	33.0	98.4
YPK−Mg^{2+}−PEP−FBP	13.4	25.5	5.6	19.0	34.6	98.2	19.6	19.9	5.7	18.8	34.1	98.1
YPK−Mg^{2+}−MgADP	18.5	20.5	5.6	18.7	33.9	97.3	21.0	18.8	5.7	18.6	33.7	97.7
YPK−Mg^{2+}−MgADP−PEP	nd[b]	nd[b]	nd[b]	nd[b]	nd[b]		22.9	17.4	5.7	18.3	33.1	97.3

[a] Deconvolution of the CD spectra acquired for wild-type and T298C YPK was performed using *CD Spectroscopy Deconvolution Program*, version 2.1 (*30*) (see the Supporting Information for details). The average error of predicted secondary structures of the network used to train the program is 6.6%. YPK refers to yeast pyruvate kinase (0.05 mg/mL) in the presence of 200 mM KCl. [b] Not determined.

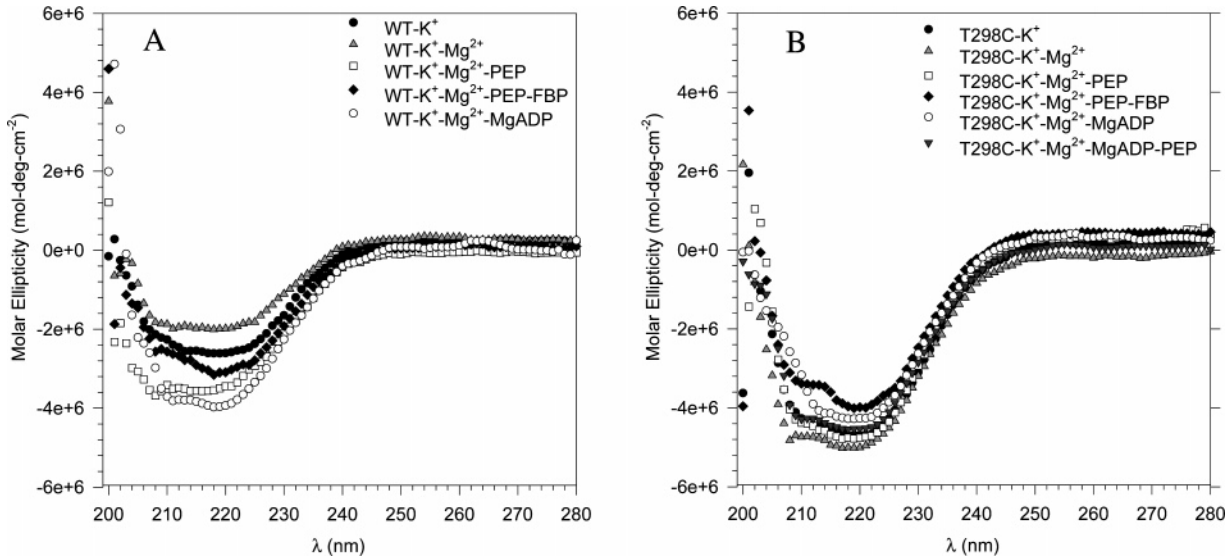

FIGURE 6: CD spectra of different ligated forms of YPK. (A) CD spectra of wild-type YPK complexes. (B) CD spectra of T298C YPK complexes. The key for the symbols designating each complex is given in the inset. Final concentrations for all species were as follows: 0.05 mg/mL YPK, 200 mM KCl, 15 mM $MgCl_2$, 0.5 mM PEP, 1 mM FBP, and 0.5 mM ADP, when present.

complexes. The interactions of FBP with apo T298C and with the binary complexes are more favorable than those with wild-type YPK. The interaction of FBP with the ternary enzyme complexes has been destabilized relative to those observed with wild-type YPK. The most drastic changes are seen in the interaction of FBP with the apo T298C, T298C−Mg^{2+}, and T298C−Mg^{2+}−PEP complexes. The T298C mutation causes a stabilization of the interaction of FBP with apo YPK of 1.49 kcal/mol and of the interaction of FBP with the YPK−Mg^{2+} complex of 1.33 kcal/mol and a destabilization of the interaction of FBP with the YPK−Mg^{2+}−PEP complex of 1.45 kcal/mol relative to wild-type YPK. Destabilization of the interaction of PEP with the YPK−Mn^{2+} complex and of the interaction of Mn^{2+} with the YPK−PEP complex is by 1.92 and 1.5 kcal/mol, respectively, relative to wild-type YPK. The quaternary T298C−Mg^{2+}−PEP−MgADP complex does form, and ligand binding is quantified.

Circular Dichroism Spectroscopy. CD spectra were measured to assess any structural differences between wild-type and T298C YPK enzymes. A comparison of the CD spectra for T298C and for wild-type YPK (Figure S.6A−E of the Supporting Information) for the YPK (apo YPK), YPK−Mg^{2+}, YPK−Mg^{2+}−PEP, YPK−Mg^{2+}−PEP−FBP, and YPK−Mg^{2+}−MgADP complexes indicates significant spectral differences between wild-type and T298C YPK for the YPK−Mg^{2+} and YPK−Mg^{2+}−PEP complexes (Figure S.6A,B). These differences are attributed to the content of α-helices and antiparallel β-sheets between wild-type and T298C YPK complexes as calculated from deconvolution (Table 7). The CD spectra of various ligated forms of wild-type YPK are shown in Figure 6A. The spectra of each of the wild-type complexes are slightly different from each other, suggesting that formation of these ligated forms of the enzyme involves conformational responses reflected as apparent differences in secondary structure (see Table 7 for differences in calculated secondary structure elements). Figure 6B displays the CD spectra for various ligated forms of T298C YPK. The CD spectra of apo T298C and its complexes with Mg^{2+}, PEP, and MgADP are similar, suggesting similar conformations for these ligated forms of T298C YPK. These data are consistent with the binding and kinetic results obtained with T298C with Mg^{2+}. The binding of Mg^{2+} followed by binding of MgADP and of PEP to T298C YPK does not introduce a significant change in the secondary structure (conformation) of the enzyme, in contrast to the CD spectral changes detected for wild-type YPK. Subsequent binding of FBP to the YPK−Mg^{2+}−PEP ternary complex of T298C YPK results in major structural changes in the enzyme and consequent catalytic activity.

Solvent Isotope Effects on the YPK-Catalyzed Reaction. Solvent isotope effect (SIE) studies were undertaken with wild-type and T298C YPK in the absence and presence of FBP to assess the role of water in catalysis by YPK. SIEs

Table 8: Solvent Isotope Effects for Wild-Type and T298C YPK[a]

complex	solvent[b]	k_{cat} (min^{-1})	$K_{m,PEP}$ (μM)	$k_{cat}/K_{m,PEP}$ ($\times 10^6$ M^{-1} min^{-1})	$^D(k_{cat})$	$^D(k_{cat}/K_{m,PEP})$
wt−Mn^{2+}−PEP	H_2O	3470 ± 90	nd[c]	nd[c]	3.5 ± 0.2	nd[c]
wt−Mn^{2+}−PEP	D_2O	1010 ± 40	nd[c]	nd[c]		nd[c]
T298C−Mn^{2+}−PEP	H_2O	293 ± 15	nd[c]	nd[c]	1.6 ± 0.1	nd[c]
T298C−Mn^{2+}−PEP	D_2O	186 ± 11	nd[c]	nd[c]		nd[c]
wt−Mn^{2+}−PEP−FBP	H_2O	3470 ± 110	12.4 ± 1.7	280 ± 9	2.7 ± 0.1	2.2 ± 0.4
wt−Mn^{2+}−PEP−FBP	D_2O	1300 ± 30	10.3 ± 1.2	126 ± 15		
T298C−Mn^{2+}−PEP−FBP	H_2O	283 ± 4	57.9 ± 4.1	4.89 ± 0.35	1.5 ± 0.03	2.1 ± 0.2
T298C−Mn^{2+}−PEP−FBP	D_2O	188 ± 2	81.9 ± 4.2	2.29 ± 0.12		
wt−Mg^{2+}−PEP	H_2O	7000 ± 240	nd[c]	nd[c]	4.3 ± 0.3	nd[c]
wt−Mg^{2+}−PEP	D_2O	1630 ± 95	nd[c]	nd[c]		nd[c]
wt−Mg^{2+}−PEP−FBP	H_2O	13600 ± 190	112 ± 6	121 ± 7	5.2 ± 0.1	2.4 ± 0.2
wt−Mg^{2+}−PEP−FBP	D_2O	2610 ± 40	52.3 ± 4	50 ± 4		
T298C−Mg^{2+}−PEP−FBP	H_2O	1080 ± 30	4490 ± 310	0.24 ± 0.02	2.4 ± 0.1	1.8 ± 0.2
T298C−Mg^{2+}−PEP−FBP	D_2O	452 ± 7	3390 ± 130	0.13 ± 0.01		

[a] Reaction conditions were as follows: pH 6.2 (pD 6.2 in D_2O), 4 mM Mn^{2+}, 5 mM ADP, 1 mM FBP for both wild-type and T298C YPK, and 15 mM Mg^{2+} for wild-type and 20 mM Mg^{2+} for T298C. For the fixed substrate measurements in the absence of FBP, the concentration of PEP was saturating at 5 mM in the presence of Mn^{2+}, and was 15 mM in the presence of Mg^{2+}. [b] Protium was exchanged with deuterium by dissolving reagents in D_2O followed by lyophilization. This was repeated three times. The pH was adjusted with either DCl or KOD according to the relation pD = meter reading + 0.4. [c] Not determined.

were measured with Mn^{2+} and with Mg^{2+} as the divalent activator and with PEP as the variable substrate. The results of these studies are summarized in Table 8.

For the Mg^{2+}-activated YPK and in the absence of FBP, there is a significant isotope effect on k_{cat} with wild-type YPK ($^Dk_{cat} = 4.3 \pm 0.3$). Measurement of a SIE with T298C YPK was not possible due to a lack of catalytic activity under these conditions (vide supra). With Mg^{2+}-activated wild-type YPK, the presence of FBP increases the SIE on k_{cat} to 5.2 ± 0.1. The SIE on k_{cat} measured with Mg^{2+}-activated T298C YPK in the presence of FBP is 2.4 ± 0.1. There is a measurable deuterium isotope effect on $k_{cat}/K_{m,PEP}$, $^D(k_{cat}/K_{m,PEP})$, with both wild-type (2.4 ± 0.2) and T298C YPK (1.8 ± 0.2) with Mg^{2+} and in the presence of FBP (Table 8).

For the Mn^{2+}-activated YPK in the absence of FBP, the SIEs measured for k_{cat} with wild-type and T298C YPK were 3.5 ± 0.2 and 1.6 ± 0.1, respectively. The presence of FBP decreases $^Dk_{cat}$ to 2.7 ± 0.1 for wild-type YPK and has a small effect on $^Dk_{cat}$ with T298C YPK ($^Dk_{cat} = 1.5 \pm 0.03$). The SIEs on $k_{cat}/K_{m,PEP}$ measured for the Mn- and FBP-activated YPK were 2.2 ± 0.4 and 2.1 ± 0.2 with wild-type and T298C YPK, respectively. The $^Dk_{cat}$ effects are smaller with T298C YPK than with wild-type YPK. With both wild-type and T298C YPK, the values for $^Dk_{cat}$ are divalent metal-dependent, while the values for $k_{cat}/K_{m,PEP}$ are metal-independent (Table 8).

Proton Inventory on the YPK-Catalyzed Reaction. Since both wild-type and T298C YPK show significant solvent isotope effects on k_{cat}, proton inventory studies were conducted with these enzymes. These studies can permit the dissection of the reactant-state and transition-state contributions to the observed isotope effect into the individual values of fractionation factors (ϕ^R and ϕ^T). Proton inventory studies were performed on the Mg^{2+}- and Mn^{2+}-activated forms of wild-type and T298C YPK in the presence of FBP.

The proton inventory with the Mg^{2+}- and FBP-activated wild-type YPK is linear (Figure 7A), and the data were fit to eq 12. The linearity suggests that with wild-type YPK the measured isotope effect on k_{cat} of 5.2 arises from a single proton with a transition-state fractionation factor, ϕ^T, of 0.13 ± 0.03 and a reactant-state fractionation factor, ϕ^R, of ∼1 (Table 9). The Mg^{2+}- and FBP-activated T298C YPK shows a downward curvature in the proton inventory plot for k_{cat} (Figure 7A). This shape is indicative of some form of inverse isotope effect contribution to the net effect. The data with T298C YPK in Figure 7A were fit to eq 13. The calculated fractionation factors are as follows: $\phi^T = 0.15 \pm 0.01$ and $\phi^R = 0.26 \pm 0.02$ (Table 9). The inverse contribution arises from the reactant state (binding a proton weaker than bulk water does). Alternatively, the nonlinear proton inventory data for T298C can be fit assuming that the inverse contribution comes from transition-state fractionation factors $\{V_n/V_0 = [1 + n(\phi_1^T - 1)][1 + n(\phi_2^T - 1)]\}$. If this model is used, a comparable good fit is obtained with the following: $\phi_1^T = 0.36 \pm 0.03$ and $\phi_2^T = 1.68 \pm 0.07$. In this model, one fractionation factor is significantly <1 whereas the value for the second fractionation factor is >1, indicating perhaps a hindered proton in the transition state that binds tighter than in bulk water.

The proton inventories with the Mn^{2+}- and FBP-activated wild-type and T298C YPK are linear (Figure 7B). The data are fit to eq 12. The calculated fractionation factors, ϕ^T, are 0.27 ± 0.02 and 0.67 ± 0.01 for wild-type and T298C YPK, respectively (Table 9).

The fractionation factors are significantly <1, and their values are metal-dependent. Such low fractionation factors are distinct and suggest that the proton responsible for the observed overall isotope effect may be derived from a metal-bound water (*17*).

For the purposes of comparison, Table 9 summarizes the theoretical values for the solvent isotope effect on k_{cat} along with the experimentally measured values. The theoretical values for $^Dk_{cat}$ were obtained from the ratio of the experimentally measured value for k_{cat} in H_2O ($n = 0$), $(k_{cat})_0$, and the fitted value for k_{cat} in D_2O ($n = 1$), $(k_{cat})_1$, fit to eq 12 or 13.

DISCUSSION

Threonine 298 is located at the active site of pyruvate kinase, based on the recent X-ray crystal structures of both the yeast (*8*) and muscle enzymes (*9*, *24*). The orientation of T298 relative to the 2-*si* face of PEP, determined by

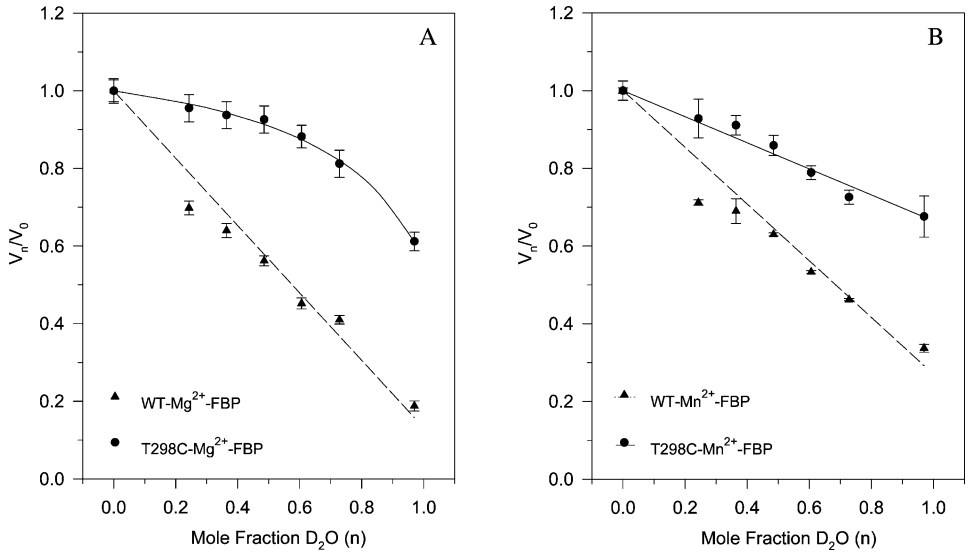

FIGURE 7: Proton inventory plots of k_{cat} for wild-type and T298C YPK. (A) Proton inventories for Mg^{2+}- and FBP-activated wild-type (▲) and T298C (●) YPK. The lines represent the best fit of the data to eq 12 for wild-type YPK and to eq 13 for T298C YPK. (B) Proton inventories for Mn^{2+}- and FBP-activated wild-type (▲) and T298C (●) YPK. The lines through the data represent the best fit to eq 12. Error bars in the data represent deviations from replicate determinations. The best-fit parameters are listed in Table 9. Wild-type and T298C YPK were assayed in a series of isotopically mixed water solutions ($[^1H]H_2O$ and $[^2H]H_2O$) with a deuterium molar fraction *n*. Initial velocities were measured at pL 6.2 (L = H or D) and at saturating concentrations of substrate PEP and of all ligands. With wild-type YPK, the concentrations of all species were as follows: 5 mM PEP, 4 mM Mn^{2+} or 15 mM Mg^{2+}, 5 mM ADP, 1 mM FBP, and 200 mM KCl. With T298C YPK, the concentrations of all species were as follows: 5 mM PEP (in the presence of Mn^{2+}) or 20 mM PEP (in the presence of Mg^{2+}), 4 mM Mn^{2+} or 20 mM Mg^{2+}, 5 mM ADP, 1 mM FBP, and 200 mM KCl. In panels A and B, each point represents the average of duplicate measurements with wild-type YPK and the average of three measurements with T298C YPK.

Table 9: Proton Inventories for Wild-Type and T298C YPK[a]

YPK complex	$^Dk_{cat}$[b]	$^Dk_{cat}$[c,d]	ϕ^T[c]	ϕ^T, ϕ^R[d]
wt−Mg^{2+}−PEP−FBP	5.2 ± 0.1	7.69 ± 1.77	0.13 ± 0.03	
T298C−Mg^{2+}−PEP−FBP	2.4 ± 0.1	1.73 ± 0.18		0.15 ± 0.01
				0.26 ± 0.02
wt−Mn^{2+}−PEP−FBP	2.7 ± 0.1	3.68 ± 0.28	0.27 ± 0.02	
T298C−Mn^{2+}−PEP−FBP	1.5 ± 0.03	1.50 ± 0.03	0.67 ± 0.01	

[a] The measurements were performed as described previously (*10*) at a fixed saturating concentration of PEP (5 mM with the wild type and Mn^{2+}-activated T298C and 20 mM with Mg^{2+}-activated T298C) and in the presence of FBP (1 mM). The final concentration of all species was saturating. [$MgCl_2$] = 15 mM with the wild type and 20 mM with T298C YPK. [$MnCl_2$] = 4 mM. [ADP] = 5 mM. [b] Values obtained from the ratio of k_{cat} in H_2O to k_{cat} in D_2O. [c] Values determined from the fit of $V_{max,app}$ to eq 12. [d] Values determined from the fit of $V_{max,app}$ to eq 13.

modeling PEP relative to phosphoglycolate or pyruvate, suggests a putative role of this residue in the enzyme-catalyzed protonation of enolpyruvate. The pyruvate kinase-catalyzed protonation of enolpyruvate has been extensively and elegantly studied by Rose and colleagues (*3*−*6*). The nature of the protonation step in the reaction catalyzed by YPK was initially addressed by mutation of residue T298 to serine and to alanine (*10*). The physical and kinetic characterization of the T298S and T298A mutants of YPK led to the conclusion that T298 is not the ultimate proton donor. The results were interpreted in a way that water is the direct proton donor and that this water is part of a proton relay that involves T298 at the active site. One of the water molecules of the proton relay is a ligand to the divalent metal ion at the catalytic site. The elimination of the alcohol functional group in the T298A mutant causes a loss of a $pK_{a,2}$ of 6.4 for k_{cat} measured for wild-type YPK and T298S. On the basis of these results, a $pK_{a,2}$ of 6.4 could be interpreted as the microscopic ionization constant of the group at position 298 or as the pK_a of some group that is important in catalysis that is influenced by the presence of T298. To address this question, the alteration of the alcohol functional group to a thiol group on T298 was undertaken. There are two advantages to the T298C mutation; sulfur is isoelectronic with oxygen, and this mutation introduces a reactive nucleophile in the active site of YPK. Physical and kinetic characterization of T298C YPK can help to further clarify the catalytic process of YPK and the nature of the protonation step.

The kinetic properties of T298C were altered relative to those of wild-type YPK. One striking effect is that with Mg^{2+} as the divalent activator, T298C YPK has an absolute requirement for the heterotropic activator FBP for catalytic activity (Table 1). An increase in the total concentration of $MgCl_2$ to 30 mM and of PEP to 20 mM in the absence of FBP did not elicit activity (<0.1 unit/mg). These results can have two possible interpretations. In the absence of FBP, substrate MgADP, PEP, or both do not bind to their respective binary enzyme complex. Alternatively, both substrates bind to the enzyme, but this is not sufficient to induce the "active" conformation at the catalytic site of T298C YPK in the absence of FBP. In either situation, binding of FBP may be sufficient to induce the appropriate conformational change at the active site of T298C YPK. Long-range interactions between the allosteric site and the active site have previously been documented in YPK (*8*).

Fluorescence emission spectra of T298C sequentially titrated with Mg^{2+}, ADP, and PEP and with Mg^{2+}, PEP, and ADP (Figure 4) indicate that MgADP and PEP both bind to the T298C−Mg^{2+} binary complex. MgADP binds with similar affinity to the YPK−Mg^{2+} binary complex of the wild type and T298C. Binding of PEP to the YPK−Mg^{2+} complex is 2 times tighter with T298C than with wild-type YPK (Table 5). The formation of the quaternary YPK−Mg^{2+}−PEP−MgADP complex of T298C is also observed. The fluorescence quenching upon formation of the YPK−Mg^{2+}−MgADP complex is different with wild-type (17%) and T298C YPK (23%), suggesting slightly different conformations surrounding the single tryptophan in the enzyme. This observation is in agreement with the results from CD spectroscopy.

CD spectra of various ligated forms of T298C YPK show that binding of Mg^{2+} and subsequent binding of MgADP, PEP, or both substrates does not introduce a significant change in the CD spectra of the mutant enzyme (Figure 6B). Subsequent binding of FBP to the T298C−Mg^{2+}−PEP complex results in major spectral changes in the mutant enzyme. This behavior is different from that observed with wild-type YPK. The spectra of all complexes are slightly different from each other, suggesting small but significant structure rearrangements upon formation of the respective ligated forms of wild-type YPK (Figure 6A). Collectively, the fluorescence emission and ligand binding studies and the CD spectroscopy analysis suggest that the lack of activity by T298C YPK with Mg^{2+} and in the absence of FBP is not due to the lack of substrate (MgADP and/or PEP) binding but due to the lack of an appropriate conformational change at the active site upon substrate binding. This conformational change must be required for catalysis. Qualitative differences in CD spectra of various ligand complexes of wt and the R49K, R49M, and R49E mutants of YPK, all of which are catalytically active, have also been observed.[2]

Mn^{2+}/Mg^{2+} mixed-metal steady-state kinetic studies with T298C YPK in the absence of FBP (Table S.2 of the Supporting Information) show that enzyme-bound Mn^{2+} or nucleotide-bound Mn^{2+} is sufficient for introduction of measurable kinetic activity with the mutant enzyme. The two divalent activators, Mn^{2+} and Mg^{2+}, when enzyme-bound, have a different effect on the interaction of MnADP with T298C YPK in the absence of FBP (Tables 2 and S.2). The interaction of MnADP with the Mn^{2+}-activated T298C is hyperbolic ($n_H = 1$, Table 2), whereas with the Mg^{2+}-activated T298C, the apparent interaction is sigmoidal ($n_H = 3.5$, Table S.2). The apparent K_m for MnADP is 2-fold lower with the Mg^{2+}-activated T298C (190 ± 4 μM) than with the Mn^{2+}-activated T298C (409 ± 16 μM). These observations suggest that there is communication between the enzyme-bound divalent metal and the nucleotide-bound Mn^{2+} at the active site of T298C YPK in the absence of FBP. This communication is different with Mn^{2+} and with Mg^{2+} as the enzyme-bound metal.

The presence of FBP restores the catalytic activity of the Mg^{2+}-activated T298C to approximately 20% of that of wild-type YPK (Table 1). With Mn^{2+} as the divalent activator, T298C YPK is kinetically similar to wild-type YPK. The Mn^{2+}-activated T298C in the absence of FBP displays homotropic kinetic cooperativity with PEP, although to a lesser extent than that observed with Mn^{2+}-activated wild-type YPK (Table 1). The presence of the heterotropic activator FBP abolishes the kinetic cooperativity with PEP in both wild-type and T298C YPK.

Alteration of the alcohol group on T298 to a thiol group causes a decrease in $k_{cat}/K_{m,PEP}$ of up to 2 orders of magnitude, indicating that T298 plays an important role in the interaction of PEP with the enzyme. The covalent radii of oxygen and sulfur are 0.73 and 1.02 Å, respectively. Hence, replacement of the hydroxyl functional group with a thiol group on the residue at position 298 may result in conformational changes around the bound PEP substrate in the active site. The T298C mutation does introduce significant conformational alterations of the substrate and the cations at the active site of YPK, as measured by $^{205}Tl^+$ NMR (*25*). The interaction of FBP with the fully ligated kinetic complex of YPK is also affected by the T298C mutation (Table 1). This reinforces the presence of long-range interactions between the active site and the regulatory site in YPK.

The pH profile for k_{cat} is changed in T298C relative to that in wild-type YPK (Figure 2). The ascending limb of the pH curve has a slope of 1 with the wild type and is doubled with T298C YPK, indicating the ionization of two groups in this pH region with the mutant enzyme. Alteration of the alcohol group on T298 to a thiol group causes an acidic shift of pK_B for k_{cat} from 6.4 to 5.5 (Table 3). Elimination of the functional group at position 298 results in the loss of the pK_B of 6.4. It is this ionization that is responsible for modulation of k_{cat} in the YPK-catalyzed reaction. Thus, Thr 298 can be considered a candidate for pK_B, since physical and kinetic characterizations of the T298 mutants indicate an important although not critical role for this residue in catalysis of YPK. It may be feasible that pK_B is the microscopic ionization constant of the group at position 298, threonine or cysteine, although this interpretation requires caution. The residue at position 298 may influence the pK_a of some other residue that is important in catalysis. S-Carboxymethylation of Cys 298 is pH-dependent, and the rate of inactivation increases with an increase in pH (Figure 3B). A pK_a of 8.2 is measured for Cys 298 in the free enzyme from the chemical modification with iodoacetate. This value is consistent with a pK_a of an isolated cysteine residue (pK_a = 8.3). Comparison of these data with results obtained by steady-state kinetics of T298C YPK (Table 3) shows no ionization in the k_{cat} versus pH profile that corresponds to this residue. Consequently, the pK_B in the k_{cat} versus pH profile does not appear to represent the microscopic ionization constant of the residue at position 298 in YPK. The presence of a hydrogen bond donor or acceptor at position 298 provides a pK_B that modulates k_{cat}, indicating that this residue affects an ionization, perhaps of water, that affects the catalytic process. The S-carboxymethyl form of T298C has a residual 15% activity, which is pH-independent, further indicating that, despite steric effects, the residue at position 298 influences YPK catalysis.

Wild-type YPK is also inactivated by iodoacetate in a pH-dependent manner (Figure 3A), although with a significantly slower rate than T298C YPK. The inactivation of T298C YPK by iodoacetate was corrected for the background inactivation of wild-type YPK by this reagent. With wild-

[2] T. Maxwell and T. Nowak, unpublished observations.

type YPK, the pK_a calculated from the pH dependence of the rate constant of inactivation by iodoacetate is 8.7 ± 0.1. This value is the same as pK_C (8.8 ± 0.2) from the kinetic studies with wild-type YPK. The pK_C of 8.8 is attributed to Lys 240, an active site residue shown to play an important role in stabilization of the pentavalent transition state of the phosphoryl group undergoing transfer (*7*). The chemical modification of Lys 240 by iodoacetate would not be surprising. Reactive, neutral Lys residues have been documented to be good nucleophiles for iodoacetate (*26*).

Solvent isotope effects (SIEs) on k_{cat} and $k_{cat}/K_{M,PEP}$ for wild-type and T298C YPK were measured to address the role of solvent in the rate-limiting step of the YPK-catalyzed reaction. There are measurable SIEs on k_{cat} and $k_{cat}/K_{M,PEP}$ for both wild-type and T298C YPK (Table 8), suggesting that the solvent water plays an important role in PEP binding and in catalysis by YPK. The isotope effects are smaller with T298C YPK than with wild-type YPK regardless of the divalent metal activator. The effect of the T298C mutation on $^D(k_{cat}/K_{M,PEP})$ is similar to that for wild-type YPK, and the effects are modest. These results suggest that the mutation at T298 does not play a critical role in the solvent-sensitive steps up to and including the first irreversible step. The first irreversible step is most likely phosphoryl transfer. Assuming that the isotope-sensitive step in the net reaction is the same in wild-type and T298C YPK, these results indicate that T298 primarily affects a later step that involves proton transfer and occurs after phosphoryl transfer in net catalysis. With both wild-type and T298C YPK, the values for $^D(k_{cat})$ are divalent metal-dependent; $^D(k_{cat}/K_{M,PEP})$ values are metal-independent (Table 8). Mg^{2+}-activated YPK gives a larger SIE on k_{cat} than Mn^{2+}-activated YPK. This suggests that the divalent metal plays a role in a solvent-sensitive step in the net reaction catalyzed by YPK. It has been observed that deletion of the cationic groups of Lys 240 (*7*) and Arg 49[2] that facilitate phosphoryl transfer results in SIE values of 1. Thr 298 or Cys 298 plays an important role in enolpyruvate protonation; Lys 240 and Arg 49 function in phosphoryl transfer.

The fractionation factors (ϕ) measured with YPK change with the mutation of Thr 298 to cysteine and are metal-dependent (Table 9). With both wild-type and T298C YPK, the fractionation factor is significantly less than 1, suggesting that ^1H and not ^2H accumulates at the site of exchange in the transition state. Values of <1 for the fractionation factors have been identified with cysteine residues ($\phi = 0.40-0.60$) or with metal-bound water (an average $\phi = 0.64$) (*17*). Most other functional groups, including alcohols, have a ϕ of 1.0. In the active site of wild-type YPK, there is no cysteine residue, nor is there any evidence that such a residue plays a role in PK catalysis. In T298C YPK, a cysteine residue has been introduced into the active site of the enzyme. A fractionation factor of significantly less than 1 has been measured for both wild-type YPK that does not have this cysteine and the T298A YPK mutant, where the functional group at position 298 was removed (*10*). This indicates that the ϕ of <1 measured with T298C is not due to Cys 298. Hence, the fractionation factors of <1 measured with wild-type YPK and T298 mutants, including T298C, indicate that the proton that is important in the solvent-sensitive step originates from a metal-bound water. This conclusion is supported by the metal dependency of the fractionation factors measured with wild-type YPK and the T298 mutants.

The single tryptophan residue per subunit of YPK, W452, is used as an intrinsic fluorescent probe to measure the extent of ligand binding in both the wild type and T298C. Because T298C YPK does not undergo steady-state turnover in the presence of Mg^{2+} and in the absence of FBP, it was possible to assess the binding of MgADP to the T298C$-Mg^{2+}$ and T298C$-Mg^{2+}-$PEP complexes and of PEP to the T298C$-Mg^{2+}-$MgADP complex. The ligand dissociation constants measured are thermodynamic parameters and are related directly to the binding free energies. When cooperativity in binding is observed, the value that is calculated for K_D using eq 10 is an apparent value. From this treatment, the ligand concentration giving half-maximal binding is obtained. To relate $K_{D,app}$ to a thermodynamic value, these data are fit to a model that relates to an intrinsic binding constant at the site of the protein. Such a treatment requires coupling factors for binding. A rapid equilibrium model describing the cooperative binding of a substrate to an enzyme with four equivalent binding sites was developed by Thomas Bollenbach (*11*) and was used herein to fit the fluorescence data for T298C when cooperativity in binding was observed. The $K_{D,app}$ and K^*_D (intrinsic dissociation constant) values resulting from this treatment of the ligand binding data with T298C are listed in the Supporting Information (Table S.3), along with the corresponding standard free energies of formation of the respective YPK complexes (ΔG^*). It should be noted that the ΔG^* values are different from the apparent ΔG values presented in Tables 5 and 6. The ΔG^* values, calculated for cooperative ligand binding (Table S.3), are assumed to reflect actual thermodynamic values. ΔG^* and the ΔG values determined for hyperbolic ligand binding (Tables 5 and 6) were used to calculate the two- and three-ligand coupling free energies listed in Table S.4 (Supporting Information). This thermodynamic linked-function analysis allows for the quantitation of the heterotropic multiligand interactions that occur between PEP, divalent metal, and FBP and YPK (wild type and T298C) in the absence of the metal−nucleotide substrate. Detailed thermodynamic linked-function analyses have been used previously to study these interactions with wild-type YPK (*21*, *23*). This analysis is based on general principles outlined by Wyman (*27*) and Weber (*28*, *29*) and was described in detail elsewhere (*21*).

The following analysis is based on the data listed in Tables S.3 and S.4 (Supporting Information). (a) $\Delta(\Delta G_{Mg-PEP})$, the two-ligand coupling free energy for coupling of Mg^{2+} and PEP to T298C, is weak, and the calculated values differ by 0.84 kcal/mol, depending on the order of addition of the ligands to the enzyme (Table S.4). Since true thermodynamic constants were used for calculation of $\Delta(\Delta G_{Mg-PEP})$, the difference in the value suggests that the T298C$-Mg^{2+}-$PEP complexes that form depend on whether Mg^{2+} or PEP binds first to apo T298C. If Mg^{2+} binds first, $\Delta(\Delta G_{Mg-PEP}) = +0.57 \pm 0.04$ kcal/mol. If PEP binds first, $\Delta(\Delta G_{Mg-PEP}) = -0.27 \pm 0.07$ kcal/mol. These results suggest that pre-equilibration of the mutant enzyme in the presence of saturating concentrations of Mg^{2+} or PEP will generate different forms of the enzyme, each of which stabilizes subsequent ligand binding to a different extent. This dependence on the order of ligand binding is supported by the different fluorescent emission spectra upon formation of the T298C$-Mg^{2+}-$PEP (Figure S.3A) and T298C$-$PEP$-Mg^{2+}$

(Figure 4A) complexes. It is also possible that one of these complexes may not be kinetically competent.

(b) $\Delta(\Delta G_{Mn-PEP})$, the free energy for coupling between Mn^{2+} and PEP, is weak for T298C (-0.43 ± 0.02 kcal/mol) compared to that of wild-type YPK (-3.88 ± 0.08 kcal/mol) (Table S.4). The relatively large cooperative interaction between Mn^{2+} and PEP in wild-type YPK was attributed to the formation of a strong inner sphere coordination complex between the enzyme-bound Mn^{2+} and the phosphoryl group of PEP (*21*). In T298C, it is possible that the extent of the electrostatic interaction between enzyme-bound Mn^{2+} and PEP is affected by the conformational alterations introduced at the active site by the mutation in the vicinity of the substrate PEP and the cations. The total free energy of formation[3] of the YPK$-M^{2+}-$PEP complex is similar in the wild type ($\Delta G'_{wt-Mg-PEP} = -7.57 \pm 0.09$ and -6.06 ± 0.16 kcal/mol; $\Delta G'_{wt-Mn-PEP} = -11.10 \pm 0.09$ and -9.73 ± 0.09 kcal/mol) and in T298C YPK ($\Delta G'_{T298C-Mg-PEP} = -7.79 \pm 0.06$ and -6.95 ± 0.07; $\Delta G'_{T298C-Mn-PEP} = -9.75 \pm 0.05$ and -9.10 ± 0.05 kcal/mol), regardless of the divalent activator.

(c) $\Delta(\Delta G_{M-FBP})$, the free energy for coupling between the divalent metal and FBP in the absence of PEP, is weaker for T298C YPK [$\Delta(\Delta G_{Mg-FBP}) = -0.14 \pm 0.04$, $\Delta(\Delta G_{Mn-FBP}) = -0.38 \pm 0.04$ kcal/mol] compared to that for the analogous interaction in wild-type YPK [$\Delta(\Delta G_{Mg-FBP}) = -0.75 \pm 0.03$ (*23*), $\Delta(\Delta G_{Mn-FBP}) = -1.09 \pm 0.02$ kcal/mol (*21*)] (Table S.4). The coupling between the divalent metal binding site and the FBP binding site is the result of structural changes in the protein backbone communicated over a long range, since the two sites are more than 40 Å apart (*8*). It is evident that Mg^{2+} and Mn^{2+} induce different structures at the FBP binding site and that these structures are different in T298C and wild-type YPK. The communication between the binding sites for the divalent metal and for FBP is changed in T298C from that in wild-type YPK.

(d) The interaction between PEP and FBP in the absence of divalent metal is weak in the wild type [$\Delta(\Delta G_{PEP-FBP}) = -0.38 \pm 0.04$ kcal/mol (*23*)] and is antagonistic in T298C YPK [$\Delta(\Delta G_{PEP-FBP}) = 1.26 \pm 0.04$ kcal/mol] (Table S.4). The values for $\Delta G_{PEP-FBP}$ were calculated assuming that PEP binds first to apo YPK. Binding of FBP to apo T298C is strongly favored over binding of PEP. In T298C, the formation of the YPK$-$FBP complex is stabilized by 1.74 kcal/mol over the formation of the YPK$-$PEP complex. In wild-type YPK, these two binary complexes are thermodynamically equally favored (Tables 5 and S.3). Kinetic measurements with the Mn^{2+}- or Mg^{2+}-activated wild type and with the Mn^{2+}-activated T298C suggest that the coupling between PEP and FBP is large. The apparent affinity of the enzyme for PEP is increased in the presence of FBP (Table 1). Previous kinetic and thermodynamic linked-function studies of the Mn^{2+}- and Mg^{2+}-activated wild-type YPK have shown that it is the enzyme-bound metal that modulates the coupling between the PEP and FBP sites (*12*, *19*, *21*, *23*). In wild-type YPK, the coupling between PEP and FBP in the presence of saturating concentrations of divalent metal is cooperative. In T298C, the coupling free energy of interaction between PEP and FBP in the presence of a saturating Mg^{2+} concentration is antagonistic and in the presence of Mn^{2+} is synergistic but weak. In T298C, Mn^{2+} but not Mg^{2+} plays the same role as in the wild type, to communicate a positive allosteric interaction between the PEP and FBP sites.

(e) The large negative $\Delta(\Delta G_{M-PEP-FBP})$ with wild-type YPK [$\Delta(\Delta G_{Mg-PEP-FBP}) = -3.21 \pm 0.03$ (*23*), $\Delta(\Delta G_{Mn-PEP-FBP}) = -6.60 \pm 0.09$ kcal/mol (*21*)] (Table S.4) indicates that the formation of the quaternary YPK$-$PEP$-M^{2+}-$FBP complex is strongly favored over the formation of other binary and ternary complexes. The formation of the T298C$-Mg^{2+}-$PEP$-$FBP complex is disfavored by 1.48 kcal/mol compared to the formation of any binary or ternary complexes with Mg^{2+}. The formation of the Mg^{2+}-activated quaternary complex is significantly less favorable due to the large positive $\Delta(\Delta G_{PEP-FBP/Mg})$ compared to the negative $\Delta(\Delta G_{PEP-FBP/Mn})$. It is important to recognize that the values for $\Delta(\Delta G_{PEP-FBP/M})$ and $\Delta(\Delta G_{M-PEP-FBP})$ are determined in the absence of the second substrate, M^{2+}ADP. In wild-type YPK, MgADP induces the homotropic cooperativity in PEP binding to the YPK$-Mg^{2+}-$MgADP complex, as determined from the binding of the slow substrate (*Z*)-3-fluoroPEP to the ternary complex (*19*). Binding of PEP to the T298C$-Mg^{2+}-$MgADP complex is hyperbolic (Table 5). It is possible that the conformation induced by MgADP at the PEP site is different in wild-type and T298C YPK, at least in the absence of FBP. The coupling between PEP and MgADP in the presence of a saturating Mg^{2+} concentration and in the absence of FBP is antagonistic in T298C ($+0.19 \pm 0.04$ kcal/mol), assuming that PEP binds first. This suggests that in T298C, binding of FBP at the regulatory site assists in inducing the "active" conformation at the active site where PEP binds. This would be true if one assumes that the formation of the T298C$-$PEP$-Mg^{2+}-$MgADP$-$FBP complex is thermodynamically favored and this complex adopts the kinetically active conformation. MgADP also appears to influence the homotropic cooperativity of FBP binding to both wild-type YPK (*19*, *23*) and T298C. FBP binds with positive cooperativity to the YPK$-Mg^{2+}-$PEP complex of both wild-type ($n_H = 1.3$) and T298C YPK ($n_H = 1.9$) (Table 5). The kinetic response of YPK to FBP is sigmoidal ($n_H = 2.6$) with T298C at saturating PEP, Mg^{2+}, and MgADP concentrations (Figure 1) but is hyperbolic with the wild type extrapolated to saturating PEP and Mg^{2+} concentrations (*19*) (Table 1). It is possible that MgADP also plays a role in modulating the communication between the PEP and FBP sites in YPK. In T298C YPK, the role of MgADP may be more important than the role of Mg^{2+}. In wild-type YPK, enzyme-bound Mg^{2+} may have the dominant role.

In conclusion, the results with T298C YPK presented in this work and data from previous studies with the T298A and T298S YPK mutants (*10*) are consistent with water from a specific channel moving into the active site of the protein, and not T298, that serves as the ultimate donor of protons to enolpyruvate in yeast PK. One of the waters in this channel is coordinated to the enzyme-bound divalent metal. Thr 298 plays a role in a late step in the catalytic mechanism that

[3] The total free energy of formation of the YPK$-M^{2+}-$PEP complex, $\Delta\Delta G'_{YPK-M-PEP}$, is defined, depending on the order of ligand binding, as the sum $\Delta G_{YPK-PEP} + \Delta G_{YPK-PEP-M}$ or the sum $\Delta G_{YPK-M} + \Delta G_{YPK-M-PEP}$. The free energies of binding (ΔG) used for the calculation of $\Delta G'_{YPK-M-PEP}$ are listed in Tables 5 and 6. Where appropriate, the ΔG^* values summarized in Table S.3 were used to compute $\Delta G'_{YPK-M-PEP}$.

involves proton transfer. These results indicate that T298 is the amino acid that interacts with the terminal water molecule that is at the end of the proton circuit. The residue at position 298 affects the pK_a of the water in the water channel and therefore its reactivity. The proposal of a water channel to the active site of PK and of a water molecule in this channel as the ultimate proton donor is supported by structural data with rabbit muscle PK (*24*) and by proton relaxation rate (PRR) data obtained with wild-type YPK and T298 mutants (*20*). The results of this work also suggest that Thr 298 is important in the interaction of the substrate PEP with the enzyme and in positioning PEP for catalysis. The studies presented herein demonstrate that the second pK_a of 5.5−6.4 in the k_{cat} versus pH profile is not the microscopic ionization constant of the amino acid residue at position 298 in YPK. The residue at position 298 in YPK affects the complex coupled ligand interactions for this allosteric enzyme.

SUPPORTING INFORMATION AVAILABLE

The procedure followed for deconvolution of the CD spectra for wild-type and T298C YPK is described. The following figures and tables are shown and are listed in the order of presentation: one figure showing the overlapped CD spectra of wild-type and T298C YPK; one figure showing the overlapped fluorescence emission spectra of wild-type and T298C YPK; one table with the parameters and statistical summary for fits of pH−rate data for T298C YPK to the three models that are described in this work; two figures showing the fluorescence emission spectra of T298C YPK and of its complexes with Mg^{2+}, PEP, and FBP and Mn^{2+}, PEP, and FBP; one figure showing the interaction of PEP with the T298C−Mn^{2+} complex, as measured by steady-state fluorescence; one figure showing the comparative CD spectra of wild-type and T298C YPK; one table with the steady-state kinetic parameters from the mixed-metal studies with T298C YPK in the absence of FBP; one table with the intrinsic dissociation constants for the interaction of Mn^{2+} and FBP with various complexes of T298C YPK; and one table with two- and three-ligand coupling free energies for Mg^{2+}- and Mn^{2+}-activated wild-type (*21*, *23*) and T298C YPK. The experimental conditions for the mixed-metal steady-state kinetic studies with T298C YPK and the mathematical treatment of the data derived from these studies are described. This material is available free of charge via Internet at http://pubs.acs.org.

REFERENCES

1. Blättler, W. A., and Knowles, J. R. (1979) Stereochemical course of phosphokinases. The use of adenosine [γ-(S)-^{16}O,^{17}O,^{18}O]-triphosphate and the mechanistic consequences for the reactions catalyzed by glycerol kinase, hexokinase, pyruvate kinase, and acetate kinase, *Biochemistry 18*, 3927−3933.
2. Rose, I. A. (1970) Stereochemistry of pyruvate kinase, pyruvate carboxylase, and malate enzyme reactions, *J. Biol. Chem. 245*, 6052−6056.
3. Kuo, D. J., and Rose, I. A. (1978) Stereochemistry of ketonization of enolpyruvate by pyruvate kinase. Evidence for its role as an intermediate, *J. Am. Chem. Soc. 100*, 6288−6289.
4. Kuo, D. J., O'Connell, E. L., and Rose, I. A. (1979) Physical, chemical, and enzymological characterization of enolpyruvate, *J. Am. Chem. Soc. 101*, 5025−5030.
5. Rose, I. A., Kuo, D. J., and Warms, J. V. (1991) A rate-determining proton relay in the pyruvate kinase reaction, *Biochemistry 30*, 722−726.
6. Rose, I. A., and Kuo, D. J. (1989) The substrate proton of the pyruvate kinase reaction, *Biochemistry 28*, 9579−9585.
7. Bollenbach, T. J., Mesecar, A. D., and Nowak, T. (1999) Role of lysine 240 in the mechanism of yeast pyruvate kinase catalysis, *Biochemistry 38*, 9137−9145.
8. Jurica, M. S., Mesecar, A., Heath, P. J., Shi, W., Nowak, T., and Stoddard, B. L. (1998) The allosteric regulation of pyruvate kinase by fructose-1,6-bisphosphate, *Structure 6*, 195−210.
9. Larsen, T. M., Laughlin, L. T., Holden, H. M., Rayment, I., and Reed, G. H. (1994) Structure of rabbit muscle pyruvate kinase complexed with Mn^{2+}, K^+, and pyruvate, *Biochemistry 33*, 6301−6309.
10. Susan-Resiga, D., and Nowak, T. (2003) The proton-transfer step catalyzed by yeast pyruvate kinase, *J. Biol. Chem. 278*, 12660−12671.
11. Bollenbach, T. J. (1999) Catalytic Mechanism and Allosteric Activation of Yeast Pyruvate Kinase, Ph.D. Thesis, University of Notre Dame, Notre Dame, IN.
12. Mesecar, A. D., and Nowak, T. (1997) Metal-ion-mediated allosteric triggering of yeast pyruvate kinase. 1. A multidimensional kinetic linked-function analysis, *Biochemistry 36*, 6792−6802.
13. Tietz, A., and Ochoa, S. (1958) Fluorokinase and Pyruvic Kinase, *Arch. Biochem. Biophys. 78*, 477−493.
14. Mesecar, A. M. (1995) Kinetic Responses and Conformational Changes Required for Yeast Pyruvate Kinase Activation and Catalysis, Ph.D. Thesis, University of Notre Dame, Notre Dame, IN.
15. Cleland, W. W. (1979) Statistical Analysis of Enzyme Kinetic Data, *Methods Enzymol. 63*, 103−138.
16. Kresge, A. J. (1964) Solvent isotope effects in H_2O-D_2O mixtures, *Pure Appl. Chem. 8*, 243−258.
17. Showen, K. B., and Showen, R. L. (1982) Solvent Isotope Effects on Enzyme Systems, *Methods Enzymol. 87*, 551−606.
18. Alder, A. J., Greenfield, H. J., and Fasman, G. D. (1973) Circular Dichroism and Optical Rotatory Dispersion of Proteins and Polypeptides, *Methods Enzymol. 27*, 675−735.
19. Bollenbach, T. J., and Nowak, T. (2001) Kinetic linked-function analysis of the multiligand interactions on Mg^{2+}-activated yeast pyruvate kinase, *Biochemistry 40*, 13097−13106.
20. Susan-Resiga, D. (2003) Proton Transfer and the Catalytic Mechanism of Yeast Pyruvate Kinase, Ph.D. Thesis, University of Notre Dame, Notre Dame, IN.
21. Mesecar, A. D., and Nowak, T. (1997) Metal-ion-mediated allosteric triggering of yeast pyruvate kinase. 2. A multidimensional thermodynamic linked-function analysis, *Biochemistry 36*, 6803−6813.
22. Kuczenski, R. T., and Suelter, C. H. (1971) Interactions of fructose 1,6-diphosphate, substrates, and monovalent cations with yeast pyruvate kinase monitored by changes in enzyme fluorescence, *Biochemistry 10*, 2862−2866.
23. Bollenbach, T. J., and Nowak, T. (2001) Thermodynamic linked-function analysis of Mg^{2+}-activated yeast pyruvate kinase, *Biochemistry 40*, 13088−13096.
24. Larsen, T. M., Benning, M. M., Rayment, I., and Reed, G. H. (1998) Structure of the bis(Mg^{2+})-ATP-oxalate complex of the rabbit muscle pyruvate kinase at 2.1 Å resolution: ATP binding over a barrel, *Biochemistry 37*, 6247−6255.
25. Susan-Resiga, D., and Nowak, T. (2003) Monitoring active site alterations upon mutation of yeast pyruvate kinase using $^{205}Tl^+$ NMR, *J. Biol. Chem. 278*, 40943−40952.
26. Lundblad, R. L. (1995) The Modification of Cysteine, in *Techniques in Protein Modification*, pp 63−89, CRC Press, Boca Raton, FL.
27. Wyman, J. (1964) Linked functions and reciprocal effects in hemoglobin: a second look, *Adv. Protein Chem. 19*, 223−286.
28. Weber, G. (1972) Ligand binding and internal equilibria in proteins, *Biochemistry 11*, 864−878.
29. Weber, G. (1975) Energetics of ligand binding to proteins, *Adv. Protein Chem. 29*, 1−83.
30. Böhm, G. (1998) *Spectroscopy Deconvolution Program (CDNN Free Software for Windows 5/98 or Windows NT)*, version 2.1.

BI049864D